UNCLASSIFIED

AD NUMBER
ADB264579
NEW LIMITATION CHANGE
TO Approved for public release, distribution unlimited
FROM Distribution authorized to U.S. Gov't. agencies only; Proprietary information; Nov 2000. Other requests shall be referred to U.S. Army Medical Research and Materiel Command, 504 Scott Street, Fort Detrick, MD, 21702-5012.
AUTHORITY
USAMRMC ltr, 23 Aug 2001

THIS PAGE IS UNCLASSIFIED

AD_____

Award Number: DAMD17-97-1-7198

TITLE: Breast Tumor Specific Peptides: Development of Breast
       Carcinoma Diagnostic and Therapeutic Agents

PRINCIPAL INVESTIGATOR: Thomas P. Quinn, Ph.D.

CONTRACTING ORGANIZATION: University of Missouri
                          Columbia, Missouri 65211

REPORT DATE: November 2000

TYPE OF REPORT: Final

PREPARED FOR: U.S. Army Medical Research and Materiel Command
               Fort Detrick, Maryland 21702-5012

20010327 078

NOTICE

THIS TECHNICAL REPORT HAS BEEN REVIEWED AND IS APPROVED FOR PUBLICATION.

REPORT DOCUMENTATION PAGE

Public reporting burden for this collection of information is estimated to average 1 hour per response, including the time for reviewing instructions, searching existing data sources, gathering and maintaining the data needed, and completing and reviewing this collection of information. Send comments regarding this burden estimate or any other aspect of this collection of information, including suggestions for reducing this burden to Washington Headquarters Services, Directorate for Information Operations and Reports, 1215 Jefferson Davis Highway, Suite 1204, Arlington, VA 22202-4302, and to the Office of Management and Budget, Paperwork Reduction Project (0704-0188), Washington, DC 20503

1. AGENCY USE ONLY (Leave blank)	2. REPORT DATE November 2000	3. REPORT TYPE AND DATES COVERED Final (1 Oct 97 - 1 Oct 00)

4. TITLE AND SUBTITLE Breast Tumor Specific Peptides: Development of Breast Carcinoma Diagnostic and Therapeutic Agents	5. FUNDING NUMBERS DAMD17-97-1-7198

6. AUTHOR(S)
Thomas P. Quinn, Ph.D.

7. PERFORMING ORGANIZATION NAME(S) AND ADDRESS(ES) University of Missouri Columbia, Missouri 65211 E-MAIL: quinnt@missouri.edu	8. PERFORMING ORGANIZATION REPORT NUMBER

9. SPONSORING / MONITORING AGENCY NAME(S) AND ADDRESS(ES) U.S. Army Medical Research and Materiel Command Fort Detrick, Maryland 21702-5012	10. SPONSORING / MONITORING AGENCY REPORT NUMBER

11. SUPPLEMENTARY NOTES

This report contains colored photos

13. ABSTRACT *(Maximum 200 Words)*

The focus of our research was to characterize the tumor imaging and therapeutic potentials of novel peptides that bound two breast tumor antigens, the pancarcinoma Thomsen-Friedenreich (T-antigen) and erbB-2 receptor. Peptides that bound T-antigen and the erbB-2 receptor were originally identified from random peptide bacteriophage display libraries. While the T-antigen binding peptide (P30) was not suitable as a radiolabeled tumor-imaging agent, it did possess remarkable anti-tumor cell adhesive properties. The P30 peptide was able to inhibit MDA-MB-435 breast carcinoma cell-cell adhesion up to 74% and tumor cell-endothelial cell adhesion by greater than 50%. The significance of T-antigen-mediated adhesion in breast cancer identifies T-antigen as a valid target for development of new anti-adhesive therapies of cancer metastases. An erbB-2 receptor binding peptide (p6.1) was also investigated as a potential breast tumor-imaging agent. We demonstrated that the p6.1 peptide selectively bound the erbB-2 receptor as well as the erbB-1 receptor, both of which are upregulated on many breast carcinomas. An analog of the p6.1 peptide, that contained an N-terminal DOTA metal chelate, was synthesized and radiolabeled. The radiolabeled [DOTA]-p6.1 conjugate bound erbB-2 positive tumor cells in vitro, but did not bind normal endothelial cells, highlighting its potential as a tumor imaging agent.

14. SUBJECT TERMS Breast Cancer , Thomsen-Friedenreich (T) antigen, ErbB-2 receptor, radiolabeled peptides, metastasis	15. NUMBER OF PAGES 81
	16. PRICE CODE

17. SECURITY CLASSIFICATION OF REPORT Unclassified	18. SECURITY CLASSIFICATION OF THIS PAGE Unclassified	19. SECURITY CLASSIFICATION OF ABSTRACT Unclassified	20. LIMITATION OF ABSTRACT Unlimited

NSN 7540-01-280-5500

Standard Form 298 (Rev. 2-89)
Prescribed by ANSI Std. Z39-18
298-102

Table of Contents

INTRODUCTION:

The focus of our DoD funded research program is to identify peptides that specifically bind two breast tumor antigens, the Thomsen-Friedenreich (T) antigen and the erbB-2 receptor. Over expression of either T antigen or erbB-2 receptor is associated with increased rates of tumor growth, tumor metastases, and reduced survival rates. A combinatorial approach was employed to identify peptides that bind T antigen and erbB-2 receptor from bacteriophage display libraries and synthetic peptide libraries. Peptides, identified from the combinatorial peptide libraries, were examined for their abilities to selectively bind T antigen and erbB-2 in vitro and on cultured breast carcinoma cells. The peptides with the best tumor cell binding properties were radiolabeled and examined for their potential to imaging tumors in mouse animal models. In addition, the T antigen binding peptides were examined for their abilities to inhibit breast tumor cell-cell homotypic adhesion and heterotypic tumor cell adhesion to endothelial cells, both important steps in cancer metastasis. The goal of this work is to better understand the critical steps in tumor metastasis and develop breast tumor-avid peptides as potential in vivo imaging or therapeutic agents.

BODY:

Task 1. *Production, purification, and structural characterization of radiolabeled P30 and MAP-P30. Label peptides either directly at the metal binding site after peptide synthesis or radiolabel peptides during peptide synthesis. Stability of radionuclide incorporation and in vitro cell binding assays. Peptide stability in serum at 37°C.*

Analogs of the T antigen binding peptides P30 (HGRFILPWWYAFSPS) and P10 (GSWYAWSPLVPSAQI) were synthesized with either an acetylated-Cys-Gly-Cys-Gly (Ac-CGCG) or Cys-Gly-Cys-Gly (CGCG) tetrapeptide appended to their amino termini (Table 1). A MAP version of P30, that contains four copies of the peptide linked via a tri-lysine tree, was also synthesized for radiolabeling experiments.

Table 1. Peptide Synthesized

Name	Peptide Sequence
Ac-CGCG-P30	Ac-CGCG-HGRFILPW**WYAFSPS**
Ac-CGCG-P54	Ac-CGCG-WHR**WYAWSP**
CGCG-P54	CGCG-WHR**WYAWSP**
Ac-CGCG-P55	Ac-CGCG-R**WYAWSP**
CGCG-P55	CGCG-R**WYAWSP**
Ac-CGCG-P10	Ac-CGCG-GS**WYAWSP**LVPSAQI
MAP-P30	A-(Lys)$_3$(HGRFILPW**WYAFSPS**)$_4$

* Putative T antigen binding sequences are highlighted in bold type.

We had previously shown that the CGCG peptide was able to coordinate $^{186/188}$Re and ^{99m}Tc when it was attached to the N-terminus of polypeptides (4). The peptides in Table 1 were synthesized on an Synergy amino acid synthesizer (P.E. Biosystems) using standard Fmoc solid phase peptide synthesis (SPPS) chemistry (4). Peptides were cleaved from the resin with a 95:5 trifluoroacetic acid (TFA):water mixture and deprotected in a 50:10:40

TFA:thioanisol:water mixture, ether precipitated, and lyophilized. Peptide preparations were purified to homogeneity on a Vydac C-18 reverse-phase (RP) column using high performance liquid chromatography (HPLC). The masses of the purified peptides were determined by fast-atom bombardment mass spectroscopy (FAB-MS). The predicted masses of Ac-CGCG-P10 and -P30 agreed with the experimentally determined values. The hydrophobic nature of the polylysine in the MAP-P30 construct made it too hydrophobic to remain in solution under physiological conditions. Therefore, we concentrated on radiolabeling the linear peptides.

The T antigen binding properties of Ac-CGCG-P10 and -P30 were examined in vitro by fluorescence quenching experiments It was important to demonstrate that the addition of the N-terminal radiometal coordination tetrapeptide did not effect T antigen binding. The K_d values for the Ac-CGCG-P10 and -P30 peptides were the same as the values determined for P10 and P30, within experimental error, indicating that the additional amino acids did not effect T antigen binding. Ac-CGCG- and CGCG- containing peptides were radiolabeled with ^{99m}Tc directly via a glucoheptonate transchelation reaction. Briefly, ^{99m}TcO VII was reduced to ^{99m}TcO V by stannous chloride in the presence of glucoheptoic acid, forming a ^{99m}TcO V-glucoheptonate complex. Peptide was added to the reaction mixture and the pH of the solution was adjusted to 7.0 with NaOH. The reaction mixture was refluxed at 80°C for 40 min. Under these conditions, the Cys sulfurs of the CGCG sequence form a more favorable ^{99m}TcO V coordination complex than glucoheptonate, which drives the peptide radiolabeling reaction. The stabilities of ^{99m}Tc labeled peptides were examined after a 24 hr incubation in phosphate buffered saline, pH 7.4 (PBS) and in PBS containing 4 mM cysteine (Table 2).

Table 2   Stability of Radiolabeled Peptides in PBS and PBS+ Cysteine 24 hr post purification.

Tc-99m-Radiolabeled Peptides	In PBS(10mM)	Cysteine(4mM)
Tc-99m-Ac-CGCG-P30	N.D.	N.D.
Tc-99m-Ac-CGCG-P10	N.D.	N.D.
Tc-99m-Ac-CGCG-P54	N.D.	40% remain
Tc-99m-CGCG-P54	N.D.	90% remain
Tc-99m-Ac-CGCG-P55	N.D.	30% remain
Tc-99m-CGCG-P55	N.D.	40% remain

*N. D.= No degradation

The radiolabeled peptides were injected on a C-18 RP column which is capable of separating labeled peptide from pertechnetate (free ^{99m}Tc). The results indicated that the ^{99m}Tc labeled peptides were stable in vitro over a 24 hr time period. In addition, the radiolabeled peptide were resistant to chemical challenges from free cysteine

Cell binding experiments were performed with cultured human breast cancer MDA-MB-435 cells (Table 3). T antigen expression on MDA-MB-435 cells was confirmed by a positive binding reaction with peanut lectin (1).

Table 3. Cell binding to MB435 for technetium labeled peptides 4°C for 1.5hr

Peptide	TB[1]	NSB[2]	SB[3]
Ac-CGCG-P30	27.7%	11.0%	16.7%
Ac-CGCG-P54	4.65%	2.23%	2.42%
Ac-CGCG-P55	1.12%	0.75%	0.37%
Ac-CGCG-P10	5.12%	4.54%	0.58%

[1]TB, total binding; [2]NSB, non-specific binding; [3]SB, specific binding.

Briefly, 2×10^6 cells were mixed with approximately 100,000 cpm of a radiolabeled peptide. The mixture was allowed to incubate at 4°C for 2 hrs. The cells were washed 2x with PBS and counted to determine total binding. Non-specific binding experiments were performed in a similar fashion except that a 1000-fold excess of unlabeled peptide was present. Specific binding was determined by subtracting the non-specific binding from total binding. The P30 and P54 peptides exhibited the highest specific binding values. In all cases, the non-specific binding was fairly high. This could be due to peptide precipitation caused by the addition of the excess cold peptide. We are repeating our binding assays in different buffers and in larger volumes to determine if peptide precipitation contributes significantly to the non-specific binding numbers.

Task 2: *Animal trials with radiolabeled P30 and MAP-P30 in nude mice breast tumor animal models. Check for clearance, biodistribution and pharmacokinetics in tumor-free and tumor-containing animals. Determine stability of peptide to proteolysis.*

The biodistribution of ^{99m}Tc labeled Ac-CGCG-P30, -P54, -P55, -P10, and CGCG-P54 and -P55 were examined in C57BL/6 normal mice. The MAP-P30 peptide was not examined in vivo due to the extreme hydrophobic nature of the radiolabeled complex. Mice were injected with 3-5 uCi of a radiolabeled peptide. At various times post injection, the mice were sacrificed and specific tissues were counted. Results from the biodistribution experiments are presented in Tables 4 and 5 as percent dose per gram or as percent of injected dose, respectively.

Table 4. Biodistribution of ^{99m}Tc-peptides in C57BL/6 normal mice 1hr post-injection reported as % injected dose/gram, (n=4±SD).

Tissue	Ac-CGCG-P30	CGCG-P54	Ac-CGCG-P54	CGCG-P55	Ac-CGCG-P55	Ac-CGCG-P10
Brain	0.09±0.02	0.02±0.02	0.02±0.02	0.01±0.02	0.02±0.01	
Blood	2.24±0.43	0.38±0.07	0.59±0.05	0.13±0.07	0.90±0.04	7.24±2.73
Heart	0.55±0.07	0.09±0.06	0.24±0.08	0.12±0.12	0.26±0.06	1.38±0.72
Lung	1.35±0.26	0.22±0.04	1.10±0.20	0.15±0.02	0.57±0.20	2.16±1.26
Liver	47.04±5.28	2.96±1.56	2.07±0.55	4.59±1.75	1.43±0.40	13.86±1.26
Spleen	1.05±0.14	0.06±0.03	0.24±0.10	0.07±0.06	0.30±0.18	0.92±0.13
Stomach	3.77±3.18	0.88±0.57	2.20±0.86	0.55±0.32	6.38±1.31	2.04±0.75
Intestines	13.60±3.05	33.53±4.40	35.27±2.94	28.24±1.39	33.74±3.97	31.49±1.45
Larger I.	1.12±1.30	3.53±5.94	23.29±37.36	5.19±6.19	33.88±22.91	0.99±0.69
Small I.	21.60±4.19	48.08±8.52	41.76±18.38	40.26±2.00	33.60±15.84	48.26±2.33
Kidneys	2.42±0.23	0.83±0.12	2.41±1.18	1.75±0.23	1.18±0.04	2.53±0.14
Muscle	0.11±0.10	0.16±0.04	0.15±0.06	0.09±0.08	0.14±0.05	0.28±0.07
Pancreas	0.50±0.12	0.63±0.50	0.29±0.09	0.08±0.05	0.32±0.04	0.74±0.24

*I.;Intestines

Results from the initial biodistribution experiments indicated that the primary route of clearance for these T antigen binding peptides was through the gastrointestinal (GI) tract. All of the peptides show low uptake in the organs around the breast (i.e. lungs and heart), except for P10 which display slightly elevated activity levels in the lungs. There was good clearance from the blood and low liver uptake for P54 and P55, while the longer peptides showed higher liver values. It was no surprise that the primary route of peptide clearance was through the GI tract given the hydrophobic nature of the P10 and P30 sequences. Removing some of the non-essential hydrophobic residues of P10 and P30 resulted in the P54 and P55 sequences. It was hypothesized that increasing the hydrophilic nature of the peptides would improve their clearance. The biodistribution patterns of the P54 and P55 peptides indicated that their was less liver uptake and better blood clearance, but the primary route of clearance was still through the GI tract. These results suggested that the hydrophobic nature of the ^{99m}Tc[Ac-CGCG] complex may have a dominant impact on the peptide's clearance properties. The presence or absence of the acetyl group on the N-terminal cysteine did not appear to have an effect on the stability of the peptides in vivo. Many peptides are rapidly proteolyzed in vivo. N-terminal acetylation affords peptides some degree of resistance to proteolysis. The fact that the N-terminal residues of the radiolabeled T antigen peptides are involved in metal coordination may prevent them from being recognized by proteases in vivo.

Table 5. Biodistribution of ^{99m}Tc-peptides in C57BL/6 normal mice 1hr post-injection reported as % injected dose, (n=4±SD).

Tissue	Ac-CGCG-P30	CGCG-P54	Ac-CGCG-P54	CGCG-P55	Ac-CGCG-P55	Ac-CGCG-P10
Brain	0.04±0.00	0.00±0.00	0.00±0.00	0.01±0.00	0.00±0.00	
Blood	3.47±0.77	0.82±0.07	0.55±0.12	1.28±0.07	0.18±0.09	0.79±0.43
Heart	0.05±0.00	0.02±0.00	0.00±0.00	0.02±0.00	0.01±0.01	0.16±0.00
Lung	0.25±0.11	0.16±0.03	0.03±0.00	0.10±0.01	0.02±0.00	0.38±0.10
Liver	49.23±1.28	2.64±0.57	3.69±2.08	1.99±0.73	5.54±2.16	16.59±1.97
Spleen	0.07±0.01	0.02±0.01	0.00±0.00	0.02±0.01	0.01±0.01	0.07±0.01
Stomach	0.62±0.45	1.05±0.29	0.33±0.15	3.78±0.09	0.21±0.11	0.38±0.14
Intestines	25.84±1.04	70.00±1.74	75.78±3.36	73.19±1.87	65.66±1.88	58.40±3.28
Large I	0.94±1.21	14.77±23.5	2.52±4.21	25.00±17.4	3.93±4.66	0.58±0.39
Small I	24.89±0.84	55.22±23.1	73.26±4.51	48.18±18.5	61.72±4.44	51.83±3.44
Kidneys	0.69±0.01	0.65±0.04	0.25±0.04	0.36±0.03	0.54±0.04	0.76±0.06
Muscle	0.01±0.01	0.01±0.00	0.01±0.00	0.01±0.00	0.00±0.00	0.03±0.00
Pancreas	0.13±0.02	0.05±0.01	0.14±0.10	0.06±0.01	0.01±0.01	0.17±0.02
Urine	15.02±0.54	20.99±2.55	17.28±1.16	1.26±0.69	26.55±1.15	9.68±0.43
Carcass	7.43±0.16	4.23±0.69	2.32±0.51	5.42±0.30	2.32±0.51	18.58±3.00

*I.;Intestines

The hydrophobic nature of the radiolabeled P-30 peptide and its shorter analogs appear to be responsible for the heptobililary/GI clearance patterns observed in vivo. The peptides were not examined in tumor bearing mice because of their poor biodistribution patterns in healthy mice.

Task 3: *Express clone of erbB-2 in frog melanophores and COS cells. Confirm expression of active protein. Screen peptide libraries for sequences that bind erbB-2. Chemically sequence the positive sequences.*

The erbB-2 extra cellular domain (ecd) gene, containing a C-terminal FLAG™ tag, engineered into the eukaryotic expression vector pRC/CMV (Invitrogen) was obtained from Dr. Fiddes at the CRC for Biopharmaceutical Research PTY LTD, Australia. This expression system was report to secrete 0.5-1 ug of erbB-2ecd/ml of culture media (2). The erbB-2ecd expression plasmid, was transfected into immortalized human embryonic kidney (HEK-293) cells. The transfected cultures were placed under geneticin selection since the erbB-2 plasmid also contained a Neo resistance gene. Individual cell clones were isolated and expanded into clonal cell lines. Culture media samples from individual erbB-2 containing KB cells lines were examined for the presence of the recombinant erbB-2 protein. The ELISA assay was developed with the chromogenic substrate p-Nitrophenyl phosphate. This ELISA assay allowed us to determine which clone was secreting the most erbB-2 protein. The identity of the secreted protein was confirmed by Western blot analysis. Clone # 7 was chosen for further amplification and protein production. The protein yields from clone # 7 nickel-chromatography purification averaged 0.8 _ g/ml of culture media. Samples of the protein were analyzed by reducing SDS-polyacrylamide gel electrophoresis (PAGE). As depicted in Figure 1, a homogeneous protein species with a molecular weight of ~95 KD was present. Approximately 80 ugs of erbB-2ecd was purified for use in phage library maturation experiments.
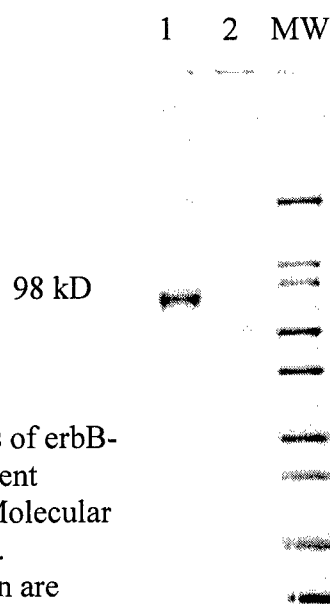
Figure 1. Analysis of erbB-2-ecd. SDS-PAGE analysis of erbB-2ecd after affinity purification. Lanes 1 and 2 are different concentrations of the purified erbB-2ecd preparation. Molecular weight markers (MW) are reported in kiloDaltons (kD). Additional details on erbB-2 expression and purification are included in manuscript #1.

Two phage display libraries, exhibiting either 15 or 6 amino acid random peptides, were screened with the purified erbB-2ecd protein. Initially, a solution of erbB-2ecd was used to coat the plates. 1 x 10^{11} phage particles from either the 15 or 6 mer library were added to the erbB-2ecd coated plates in TTBS. The plates were incubated at 25°C for 2

hrs, then washed extensively with TTBS to remove unbound phage particles. Bound phage particles were eluted from the plates in 0.1 M glycine·HCl, pH 2.2. The eluted phage were used to infect a fresh culture of E. coli to amplify the selected population used in the next round a affinity maturation. Round two began with the input phage obtained from round 1 after amplification. The same selection protocol was used as in round 1 except less biotinylated erbB-2ecd was attached to the plate. Each subsequent round of affinity maturation had less erbB-2ecd on the plate to increase the stringency of selection. In addition, neutravidin was used in round 3 and 4 instead of streptavidin to reduce non-specific binding. Table 6 lists the amount of erbB-2ecd used in each round and the input and output phage values obtained in the affinity maturation procedure.

Table 6: Affinity maturation efficiencies per round of selection.

	Round 1	Round 2	Round 3	Round 4
[biotin- erbB-2ecd] Plate coating	13 μg streptavidin	5.2 μg streptavidin	1 μg neutravidin	0.1 μg neutravidin
Inputs	6mer 1.3×10^{11} 15mer 1.3×10^{11}	6mer 1.0×10^{11} 15mer 8.0×10^{10}	6mer 1.2×10^{10} 15mer 2.8×10^{10}	6mer 6.6×10^{9} 15mer 6.0×10^{9}
Outputs	6mer 2.0×10^{4} 15mer 2.2×10^{4}	6mer 2.2×10^{5} 15mer 2.6×10^{5}	6mer 9.2×10^{4} 15mer 1.4×10^{5}	6mer 2.7×10^{6} 15mer 2.4×10^{6}
Percent yields	6mer 1.5×10^{-5} 15mer 1.2×10^{-5}	6mer 2.2×10^{-4} 15mer 3.3×10^{-5}	6mer 3.1×10^{-3} 15mer 2.0×10^{-3}	6mer 4.1×10^{-2} 15mer 3.9×10^{-2}

Phage colons obtained from round 4 of the affinity selection procedure were isolated and prepared for sequencing. First, clones from the 15mer library were sequenced. Thus far, the region of the CPIII gene encoding the random peptide inserts from 85 clones were sequenced. 95% of these clones had the same peptide amino acid sequence, Trp-Arg-Arg-Trp-Phe-Tyr-Gln-Phe-Pro-Thr-Pro-Leu-Ala-Ala-Ala. An analysis of the nucleotide sequences of the random 6-amino acid affinity selected population yielded three groups of clones. The largest group, which accounted for 75% of the sequenced clones, contained an insert encoding the KCCYSL peptide (p6.1). Within this group we found several nucleotide sequences with different bases in the third position of codons but the same amino acid sequence. This supports the fact that the peptide was selected due to peptide-protein interaction and not to propagation properties of the particular clone.

The p15 and p6.1 peptides were analyzed for stretches of homology with known protein sequences from PIR (3) and SPTREMBL (4) protein databases. FASTA (5) analysis revealed that p15 has 100% identity in 6 overlapped amino acids with the epsilon subunit of neurotransmitter receptor GABA-A and 71.4% identity in 7 overlapped amino acids with Bradikinin receptor. Although ErbB2, GABA-A receptor, and Bradikinin receptor are known to be widely expressed in the same tissues, i.e. neural, neuroglial, and epithelial. We could not reveal any reported data on possible structural similarities between GABA-A or Bradikinin receptors and the ErbB-2 protein.

A similar computer search revealed that the six-amino acid p6.1 peptide shared a limited linear sequence homology with several different proteins, including monocyte chemotactic protein (MCP), whey acidic protein (WAP), human spasmolytic protein (hSP), and the envelope protein of the Rous associated virus 1 (RAV1 Env). These

proteins, each contained five-amino acid stretches of homology to p6.1 with 1 conservative substitution (CCYTL, KCCFS, KCCFS and CCFSL respectively). Of particular interest was the homology of p6.1 with SP and RAV1 Env, since those proteins could be involved in direct interaction with ErbB receptors (6, 7). No linear sequence homology to either p6.1 or p15 was found in any of the ErbB family ligands. However, the oxidized form of p6.1 could mimic a CC(Y/F) motif formed within the EGF-like domain of all known ErbB ligands due to C_{14}-C_{31} (EGF numbering) disulfide bond (6, 7). Moreover, three of ErbB ligands, amphiregulin (AR), heregulin-α (HRG-α), and heregulin-β1 (HRG-β1), exhibit four-residue homology (KCCF) due to the presence of lysine residue next to the cysteine corresponding to C_{31} of the EGF. Since p6.1 peptide exhibited homology with several proteins, including most of the EGF like polypeptides, it was chosen for our further studies.

Task 4: *Synthesize erbB-2 binding peptides which contain a radiometal binding site. Radiolabel the peptides and examine stability of radionuclide incorporation. In vitro breast cell binding assays with erbB-2 peptides and their radiolabeled counterparts.*

The p6.1 peptide and its biotinylated analog were chemically synthesized using standard Fmoc solid phase peptide synthesis chemistry, deprotected, and purified by HPLC. Electrospray mass spectrometry was employed to confirm the molecular weight of the peptides. The binding specificity of synthetic p6.1 peptide to recombinant ErbB-2-ECD was examined by slot blot and ELISA procedures. In the slot-blot analysis, affinity purified recombinant ErbB-2-ECD and commercially available proteins: BSA, bovine asialofetuin, and human IgG were immobilized on a nitrocellulose membrane at various amounts and incubated with the biotinylated p6.1 peptide. The p6.1 peptide bound only ErbB-2 and did not react with control proteins. Fluorescence quenching experiments were performed in order to evaluate the equilibrium binding constant of p6.1 to the soluble Erb-2-ECD. Intrinsic tryptophan fluorescence of the protein was monitored as a function of peptide concentration. Since p6.1 peptide contains a tyrosine residue, samples were excited at 300 nm and monitored at 350 nm to minimize the influence of tyrosine emission on tryptophan fluorescence. Titration of ErbB-2-ECD with p6.1 resulted in substantial decrease of tryptophanyl fluorescence with maximum quenching of 20% under saturation conditions. In our analysis we assumed a model with the stoichiometric ratio of protein to peptide equal to 1:1. The data were collected at 2 uM, 4 uM and 6 uM concentrations of the protein. Theoretical curves were generated for the percentage of fluorescence quenching as a function of total peptide concentration. An apparent equilibrium dissociation constant, K_d = 30.2 +/- 7.6 uM, was determined using a nonlinear least-squares curve fitting procedure, which was applied to all three sets of data points obtained at different concentrations of protein with K_d as the shared constant for all curves. We examined the ability of the p6.1 to recognize cultured human cancer cells expressing native conformation of the ErbB-2. In double immunostaining experiments both the anti-ErbB-2 mouse monoclonal antibody [Neu (9G6)], and biotinylated p6.1 bound MDA-MB-435 breast carcinoma cells and DU-145 prostate carcinoma cells. Additional detailsand figures associated with these results can be found in the attached manuscript #1.

The erbB-2 binding peptide p6.1 was synthesized with an N-terminal DOTA metal chelate by standard Fmoc peptide chemistries. The peptide was radiolabeled with Indium-111 (^{111}In). Briefly, 20 ul of ^{111}InCl$_3$ (10 mCi/ml in 0.04 M HCl), 80 ul of 0.1 M NH$_4$OAc pH 5.5, and 10 ug of DOTA-p6.1 peptide were mixed and incubated at 70 °C for 45 min. The radiocomplex was purified via reverse phase HPLC. The purified peptide solution was purged with nitrogen to remove acetonitrile and its pH was adjusted to neutral by the addition of 0.2 M sodium phosphate (pH 8.0)/150 mM NaCl. The [^{111}In]-DOTA-p6.1 peptide was radiolabeled at high efficiency (> 95%). The [^{111}In]-DOTA-p6.1 complex was radiochemically stable in phosphate buffered saline. The ability of the [^{111}In]-DOTA-p6.1 peptide to bind erbB-2 receptor expressing MDA-MB-435 human breast and LNCap prostate carcinoma cells was examined in vitro. In initial cell binding experiments, the [^{111}In]-DOTA-p6.1 peptide bound LNCap cells with high affinity and did not bind IMR-90 normal fibroblast cells. These experiments are now being performed on the MDA-MB-435 cells.

Task 5: *In vivo testing of radiolabeled erbB-2 peptides. Determine the peptides' clearance, biodistribution and pharmacokinetic properties in tumor containing and tumor-free animals.*

Upon completion of the in vitro MDA-MB-435 cell binding experiments, we will begin the in vivo biodistribution experiments in normal and tumor bearing mice. Identification of a novel peptide that bound the erbB-2 receptor took slightly longer than we expected. In addition we have spent the last few months optimizing the synthesis and purification of the radiolabeled P6.1 complexes. Initially, we were planning to radiolabel the complexes with ^{99m}Tc using a N-terminal Ac-CGCG sequence, but based on our P30 results we felt that attaching a hydrophobic chelating sequence to p6.1 would yield a poor in vivo biodistribution pattern. Therefore, we moved to the use of the metal chelate DOTA. Unplublished biodistribution results with a DOTA-MSH peptide complex demonstrated that the DOTA moiety added to hydrophilicity to the complex and improved its biodistribution in melanoma tumor bearing mice. It is also very important that we identify the best DOTA-p6.1 complex before beginning animal work to reduce the minimize the numbers of animals used for our study. If the [^{111}In]-DOTA-p6.1 complex binds the MDA-MB-435 cells as well as the LNCap cells then we will move ahead with biodistribution experiments in normal and breast tumor bearing mice.

We recently received a NCI pre-imaging center (Pre-ICMIC) award. Tumor imaging studies with the [^{111}In]-DOTA-p6.1 complex were part of the proposal. We have the resources to complete the in vivo biodistribution work and perform initial imaging studies with [^{111}In]-DOTA-p6.1 complex.

Additional Results:

Even though the P30 peptide was not optimal as a radiolabeled tumor imaging agent, it has remarkable anti-adhesive properties. As pointed out in the original DOD proposal, we demonstrated that the P30 peptide bound the pan-carcinoma carbohydrate T antigen. In results obtained over the past 2 years, partially funded by this award, we were able to demonstrate that the P30 peptide can inhibit breast tumor cell-cell (homotypic) adhesion and breast tumor cell-endothelial cell (heterotypic) adhesion in vitro and in situ. Recent

findings demonstrate that hematogenous cancer metastases originate from intravascular growth of endothelium-attached rather than extravasated cancer cells (8), highlighting the key role of tumor-endothelial cell interactions in cancer metastasis. In this model, tumor cell endothelial cell heterotypic adhesion would be required for the initial metastatic deposit while homotypic adhesion would be important for new tumor growth. The ability of the P30 peptide to inhibit these adhesive processes has allowed us to begin to examine the metastatic process at the molecular level.

The ability of P30 to bind MDA-MB-435 breast carcinoma cells and inhibit tumor cell homotypic and heterotypic adhesion was reported in the attached manuscript #2, published in *Cancer Research*, Vol. 60, pages 2584-2588. In this manuscript we demonstrated that P30 inhibited MDA-MB-435 cell-cell adhesion in a dose dependent manner. Since T antigen contains a teminal galactose (gal) sugar residue, we investigated whether members of a gal specific lectin family, galectins, were expressed on breast tumor cells. A ^{35}S-methionine/cysteine-labeled expression profile of galectins in MDA-MB-435 cells showed that galectin 1 and galectin 3 were over expressed. It appeared reasonable that either one of these galectins or both could be involved in T-antigen mediated adhesion of tumor cells. Finally, we demonstrated that the P30 peptide could inhibit breast tumor cell-endothelial cell adhesion in a dose dependent manner upto a maximum of 50-60%. Additional experimental details are available in the attached manuscript #2.

In a second "submitted" manuscript, the molecular interactions underpinning T antigen mediated adhesion were investigated with the aid of the T antigen masking peptide P30 and a T antigen mimicking compound laculosyl L-leucine (9). In this manuscript we demonstrated that two synthetic inhibitors of T antigen-mediated adhesion, P-30 peptide, lactulosyl-L-leucine, efficiently (43-56%) inhibited the adhesion of breast and prostate cancer cells to human endothelium. Both P-30 and lactulosyl-L-leucine displayed the same maximal inhibitory effect on adhesion of breast and prostate cancer cells as a highly specific anti-T antigen monoclonal antibody did. The results of inhibition ELISA experiments confirm the specificity of both synthetic inhibitors, and demonstrated direct binding of the recombinant human galectin-3 to the protein-linked T-antigen. Remarkably, endothelial cells exhibited rapid and marked increase in cell surface galectin-3 expression when treated with T antigen-bearing glycoproteins. This result suggests a novel function for circulating T antigen-expressing glycoproteins such as cancer-associated mucin, which may act by priming capillary endothelium for harboring cancer cells. High efficiency of T antigen-mimicking and T antigen-masking inhibitors of tumor cell adhesion warrants their further development into anti-adhesive cancer therapeutics. Additional experimental details are available in the attached manuscript #3.

KEY RESEARCH ACCOMPLISHMENTS:

Identification of a novel 6 amino acid peptide from a bacteriophage display library that binds the erbB-2 receptor.

The ^{111}In-radiolabeled erbB-2 avid peptide p6.1 binds tumors cells that express the erbB-2 receptor but does not bind normal fibroblasts.

The T antigen specific P30 peptide inhibits breast tumor cell-cell adhesion as well as breast tumor cell-endothelial cell adhesion.

Galectin-3, over expressed on the surfaces of breast carcinoma cells, appears to be the preferential binding partner for T antigen.

T antigen appears to mobilize galectin-3 to the surface of endothelial cells, thus priming them for T-antigen mediated adhesion of circulating tumor cells.

Lactulosyl-L-leucine can efficiently compete off the binding of T antigen to cancer cells and T antigen-specific PNA lectin to asialofetuin.

Lactulosyl L-leucine inhibits T antigen mediated tumor cell adhesion by approximately 50%.

Both the T antigen masking P30 peptide and the T antige mimicking lactulosy L-leucine inhibit tumor cell-endothelial cell adhesion.

REPORTABLE OUTCOMES:

Manuscripts:

Karasseva, N.G., Glinsky, V.V., Chen, N.X., Komatireddy, R., and Quinn, T.P. "Identification and characterization of peptides that bind human ErbB-2 selected from bacteriophage display libraries." (manuscript in preparation, #1 Appendix I)

Glinsky, V.V., Deutscher, S.L., and Quinn, T.P.(2000) "Inhibition of human breast cancer cell aggregation and adhesion to the endothelium by T antigen-specific peptides selected from a bacteriophage display library." Poster: Era of Hope Breast Cancer Meeting, Atlanta, GA.

Glinsky, V.V., Huflejt, M.E., Glinsky, G.V., Deutscher, S.L., and Quinn, T.P. 2000. "Effects of Thomsen-Friedenreich antigen-specific peptide P-30 on β-galactoside mediated homotypic aggregation and adhesion to the endothelium of MDA-MB-435 human breast carcinoma cells." Cancer Research 60, 2584-2588. (#2 Appendix I)

Glinsky, V.V., Glinsky, G.V., Rittenhouse-Olsen, K., Huflejt, M.E., Glinskii, O.V., Deutscher, S.L., and Quinn, T.P. "The Role of Thomsen-Friedenreich Antigen in Adhesion of Human Breast and Prostate Cancer Cells to the Endothelium." (manuscript submitted, #3 Appendix I).

Funding applied for based on this work:

Funding for the development of the [DOTA]-p6.1 erbB-2 receptor-targeting peptide for imaging breast carcinoma was applied for as part of a NCI-Pre-Imaging Center (Pre-ICMIC) grant. We were awarded funding. The funding will be used to complete in vivo biodistribution and preliminary imaging studies with the radiolabeled [DOTA]-p6.1 complex.

CONCLUSIONS:

<u>P30 Peptide:</u> The P30 peptide specifically interacts with the carcinoma T antigen present on most carcinomas including breast carcinomas. The biodistribution properties of ^{99m}Tc-labeled P30 analogs, however, are not appropriate for an in vivo tumor-imaging agent. The main reasons appear to be linked to the increased hydrophobic nature of the radiolabeled complex verses the non-labeled peptide. We plan to investigate the use of a less hydrophobic metal chelate, DOTA, to radiolabel P30 and its analogs. If the DOTA-P30 conjugates are less hydrophobic then we will re-examine their biodistribution and tumor targeting properties in vivo.

The P30 peptide itself has remarkable anti-tumor cell adhesive properties. We were able to demonstrate that P30 can inhibit tumor cell-tumor cell adhesion as well as tumor cell-endothelial cell adhesion. It appears P30 inhibits tumor cell adhesion by masking T antigen, thus preventing it from participating in binding interactions with galectin-3. We were also able to demonstrate the same anti-tumor cell adhesive effects with a T antigen-mimicking agent, lactulosyl L-leucine. Both reagents were able to inhibit tumor cell endothelial cell adhesion by approximately 50%. These results demonstrate the utility of these reagents to probe the molecular underpinning of the metastatic process and highlight the potential development of T antigen inhibitors or mimetics as anti-metastatic agents.

<u>ErbB-2 receptor:</u> We were able to identify a novel peptide that binds the extra cellular domain of the ErbB-2 receptor from a random 6 amino acid peptide bacteriophage display library. We were able to demonstrate that the peptide is able to bind breast carcinoma cells (ErbB-2 positive) but does not bind T-24 human bladder carcinoma cells (ErbB-2 negative). Likewise, a ^{111}In-labeled DOTA-p6.1 peptide conjugate was able to bind ErbB-2 receptor positive tumors cells and did not bind normal human fibroblasts. The radiolabeled p6.1 complex is very soluble under physiological conditions. Once we complete our in vitro cell binding experiments, we will begin in vivo biodistribution experiments in vivo. Thus far, the results with the radiolabeled p6.1 peptide warrant further investigations of the peptide's tumor imaging properties in vivo.

REFERENCES:

1. Peletskaya, E., Glinsky, V., Glinsky, G. G., Deutscher, S. L., and Quinn, T. P. 1997. "Characterization of Peptides that Bind the Tumor-Associated Thomsen-Friedenreich Antigen Selected from Bacteriophage Display Libraries." J. Mol. Biol. 270, 374-384.

2. Clark, M.A., Hawkins, N.J., Papaionnou, A., Fiddes, R.J., Ward, R.L. (1997). Isolation of human anti-c-erbB-2 Fabs from a lymph node-derived phage display library. *Clin. Exp. Immunol.* **109**, 166-174.

3. George, D.G., Barker, W.C., Mewes, H.W., Pfeiffer, F. and Tsigita, A. (1996). The PIR international protein sequence database. *Nucl. Acids Res.*, **24**, 17-20.

4. Stoesser, G., Tuli, M.A., Lopez, R., Sterk P. (1999). The EMBL Nucleotide Sequence Database. *Nucl. Acids Res.*, **27:1**, 18-24.

5. Pearson, W.R. and Lipman, D.J. (1988). Improved tools for biological sequence comparison. *Proc. Natl. Acad. Sci.*, **85:8**, 2444-8.

6. Hynes, N.E. & Stern, D.F. (1994). The biology of *erbB-2/neu/HER-2* and its role in cancer. *Biochim. Biophys. Acta,* **1198**, 165-184.

7. McInnes, C. & Sykes, B.D. (1997). Growth factor receptors: structure, mechanism, and drug discovery. *Biopolymers,* **43:5**, 339-66.

8. Al-Mehdi, A.B., Tozawa, K., Fisher, A.B., Shientag, L., Lee, A., and Muschel, R.J. Intravascular origin of metastasis from the proliferation of endothelium-attached tumor cells: a new model for metastasis. Nat. Med. **6**, 100-102 (2000).

9. Glinsky, G.V., Mossine, V.V., Price, J.E., Bielenberg, D., Glinsky, V.V., Ananthaswamy, H.N., & Feather, M.S. Inhibition of colony formation in agarose of metastatic breast carcinoma and melanoma cells by synthetic glycoamine analogs. Clin. Exp. Metastasis **14,** 253-267 (1996).

FINAL REPORT:

Bibliography

Karasseva, N.G., Glinsky, V.V., Chen, N.X., Komatireddy, R., and Quinn, T.P. "Identification and characterization of peptides that bind human ErbB-2 selected from bacteriophage display libraries." (manuscript in preparation, #1 Appendix I)

Glinsky, V.V., Deutscher, S.L., and Quinn, T.P.(2000) "Inhibition of human breast cancer cell aggregation and adhesion to the endothelium by T antigen-specific peptides selected from a bacteriophage display library." Poster: Era of Hope Breast Cancer Meeting, Atlanta, GA.

Glinsky, V.V., Huflejt, M.E., Glinsky, G.V., Deutscher, S.L., and Quinn, T.P. 2000. "Effects of Thomsen-Friedenreich antigen-specific peptide P-30 on β-galactoside mediated homotypic aggregation and adhesion to the endothelium of MDA-MB-435 human breast carcinoma cells." Cancer Research 60, 2584-2588. (#2 Appendix I)

Glinsky, V.V., Glinsky, G.V., Rittenhouse-Olsen, K., Huflejt, M.E., Glinskii, O.V., Deutscher, S.L., and Quinn, T.P. "The Role of Thomsen-Friedenreich Antigen in Adhesion of Human Breast and Prostate Cancer Cells to the Endothelium." (manuscript submitted, #3 Appendix I).

Personnel:
Dr. Susan Deutscher, Ph.D. (Co-PI) Associate Professor
Dr. Vladislav Glinskii, M.D. Research Assistant Professor
Dr. Natalia Karasseva, Ph.D. Postdoctoral Fellow
Mr. Ravi Komatireddy, Undergraduate Biochemistry Major
Ms. Lara McKee, Undergraduate Biochemistry Major
Ms. Donna Whitner, Senior Research Technician

Appendix I

Manuscripts:
1. "Identification and characterization of peptides that bind human ErbB-2 selected from bacteriophage display libraries."
2. "Effects of Thomsen-Friedenreich antigen-specific peptide P-30 on β-galactoside mediated homotypic aggregation and adhesion to the endothelium of MDA-MB-435 human breast carcinoma cells."
3. "The Role of Thomsen-Friedenreich Antigen in Adhesion of Human Breast and Prostate Cancer Cells to the Endothelium."

Identification and Characterization of Peptides that Bind Human ErbB-2 Selected from Bacteriophage Display Libraries

Natalia G. Karasseva, Vladislav V. Glinsky, Ning X. Chen, Ravichandra Komatireddy, and Thomas P. Quinn*.

Department of Biochemistry, University of Missouri, Columbia, MO, 65211, USA.

Summary

The ErbB-2 receptor, a member of the tyrosine kinase type 1 family of receptors, has been implicated in many human malignancies, notably breast, ovarian, lung, gastric, and prostate adenocarcinomas. The overexpression of ErbB-2 in cancer cells as well as its extracellular accessibility makes it an attractive target for the development of tumor specific agents. In this study, random peptide bacteriophage display technology was employed to identify peptides that bound the extracellular domain of human ErbB-2. The peptide KCCYSL, most frequently occurring in the affinity selected population, was chemically synthesized and characterized for its binding activities to the recombinant extracellular domain of ErbB-2 using ELISA, immunoblot assays, and fluorescence quenching assays. The synthetic peptide exhibited high specificity to ErbB-2 as well as to ErbB-1, another member of ErbB family, but not to BSA, bovine asialofetuin, or human IgG. An equilibrium dissociation constant 30 μM was determined by the quenching of ErbB-2 intrinsic fluorescence upon titration with the peptide. The ability of the KCCYSL peptide to bind human breast and prostate carcinoma cells expressing different levels of the ErbB-2 receptor was demonstrated in direct cell binding assays. In conclusion, the peptide KCCYSL has the potential to

be developed into a cancer imaging or therapeutic agent targeting malignant cells overexpressing ErbB-2 receptor.

Introduction

The *erbB-2* proto-oncogene, also known as *HER-2 or neu*, is frequently altered in human cancers (Hynes & Stern, 1994). This gene encodes a 185kDa protein, denoted p185, which is also referred to as ErbB-2. ErbB-2 along with three other known homologous proteins, ErbB-1 (epidermal growth factor receptor, EGFR), ErbB-3, and ErbB-4, form the ErbB family or subclass I of receptor tyrosine kinases (RTK) (McInnes & Sykes, 1997). The activation of ErbB receptors leads to stimulation of cell growth and division. Signal transduction in this class of receptor proteins is initiated through the binding of a growth factor to the extracellular domain of the receptor, followed by receptor homo- or heterodimerization, activation of intracellular kinase domain, and tyrosine autophosphorylation (McInnes & Sykes, 1997).

The ligands for the ErbB growth factor receptor tyrosine kinase family are numerous yet similar. All of them are structurally homologous and contain an epidermal growth factor (EGF) like motif with six cysteines at highly conserved positions defining three disulfide loops that give rise to the tricyclic nature of these proteins. Despite their receptor specificity, most of the ErbB ligands are capable of binding several different receptors, thus EGF, transforming growth factor-α, and betacellulin bind ErbB-1 and the ErbB2/ErbB3 heterodimer (Alimandi et al., 1997), neuregulins associate with ErbB-3 and ErbB-4 (Jones et al., 1998), and epiregulin was shown to complex all

three receptors, i.e. ErbB-1, ErbB-3, and ErbB-4 (Shelly et.al., 1998). No ligand has been found that binds directly to ErbB-2.

Gene amplification and overexpression of ErbB-2 is associated with increased rates of tumor growth and enhanced rates of metastases (Hynes & Stern, 1994). Although ErbB-2 is also expressed at low levels in several normal organs and tissues (De Potter et al., 1989), the elevated levels of ErbB-2 in many human malignancies and its extracellular accessibility makes it an attractive target for the development of tumor-specific agents. The ErbB-2 receptor has been targeted by a variety of substances and modalities, including monoclonal antibodies (Weiner et al., 1995), immunoconjugates (Jinno et al. 1996), vaccines (Disis et al., 1999), anti-sense therapy (Wiechen et al., 1995) and gene therapy (Harris *et al.*, 1994). Recently Herceptin™, a humanized monoclonal antibody against ErbB-2 (Baselga et al., 1998), was approved for the treatment of metastatic breast cancer. Herceptin™ was shown to possess the anti-tumor activity, but it was also found to aggravate doxorubicin-induced cardiac dysfunction and, possibly, be cardiotoxic on its own (Piccart, 1999). Peptides, in contrast to large molecules like antibodies, are known to exhibit less toxicity and posses better pharmacokinetic properties such as higher target-to-background ratios and faster blood clearance (Fischman et al., 1993). Thus, in this investigation we attempted to identify peptides that specifically and tightly bound the extracellular domain (ECD) of human ErbB-2.

Advances in powerful combinatorial technologies such as bacteriophage display libraries suggest new approaches for identifying cancer-targeting molecules. Random peptide libraries can be effectively screened for sequences that bind a particular antigen or receptor. A number of peptides that bind receptor molecules (Doorbar & Winter, 1994), oncoproteins (Renschler et al., 1995),

integrins (Murayama et al., 1996), and tumor-associated carbohydrates (Peletskaya et.al., 1997, Peletskaya et.al., 1996) have been identified using bacteriophage display libraries. Bacteriophage display technology has also been employed to optimize binding affinities of heregulin variants for the ErbB3 receptor (Ballinger et al., 1998) and to study binding interactions of the heregulin-β EGF domain with ErbB3 and ErbB4 (Jones et al., 1998).

In this study, we identified three peptides from abacteriophage display library using affinity selection against recombinant ECD of human ErbB-2 (ErbB-2-ECD). One of the isolated peptides, KCCYSL (p6.1), represented 75% of selected population and exhibited limited linear homology with several proteins that potentially could interact with ErbB-1 receptor. Sequence analysis suggested that the p6.1 peptide may also act as a mimetic of a CCY/F motif present in the EGF-like domain of all known ErbB ligands. The 6-amino acid p6.1 peptide was chemically synthesized and examined for its binding affinities and specificities. Results from the binding experiments showed that the synthetic p6.1 peptide specifically recognized the recombinant ErbB-2-ECD, the ErbB-1 receptor protein, and human breast and prostate cancer cells overexpressing ErbB-2. In conclusion, our results demonstrate that the peptide p6.1 identified from a random peptide phage display library is capable of specific interaction with oncogenically activated members of the ErbB growth factor receptor family. The p6.1 peptide has the potential to be used as a vehicle for specific delivery of radionuclides or cytotoxic agents to cancer cells for therapeutical and diagnostic purposes.

Results

Purification and characterization of the recombinant extracellular domain of ErbB-2

The ECD of human ErbB-2 tagged with the FLAG epitope DYKDDDDK was expressed in

human embryonic kidney cells (HEK-293) and purified by anti-FLAG affinity chromatography

(Clark et al., 1997). The identity of the recombinant protein was confirmed by Western blot

analysis with Neu(9G6) anti-ErbB-2 mouse monoclonal antibody (Fig. 1). The purified protein

yielded a single species by SDS-PAGE analysis with molecular weight of approximately 90kDa.

However, size exclusion HPLC analysis under non-denaturing conditions revealed the molecular

weight of the recombinant ECD two fold higher than SDS-PAGE electrophoresis ~182kDa,

suggesting the existence of the protein as a homodimer in solution. This is consistent with

previously reported observations describing the ErbB-2-ECD in sera from patients with various

carcinomas as a homodimer with MW ~ 200kDa (Wu et al., 1993). The affinity purified ErbB-2-

ECD was biotinylated and used in the biopanning procedures.

Isolation of peptide sequences that bind ErbB-2 extracellular domain

A random 6- amino acid peptide bacteriophage display library was affinity selected against the

ErbB-2-ECD to identify novel peptide-ligands. The library was based on the fUSE5 bacteriophage

vector encoding the foreign peptide insert in N-terminus of minor coat protein pIII (Scott & Smith,

1990). Four rounds of affinity selection were employed to enrich phage populations for virions that

displayed peptides with affinity to ErbB-2-ECD (Table 1). The analysis of 100 clones from the

affinity selected phage population revealed three groups of clones. The largest group, which

accounted for 75% of the sequenced clones, contained an insert encoding the KCCYSL peptide

(p6.1). Within this group we found several nucleotide sequences with different bases in the third

position of codons but the same amino acid sequence. This supports the fact that the peptide was selected due to peptide-protein interaction and not to propagation properties of the particular clone. The remaining clones fell into two groups with similar sequences WYAWML (p6.2) and WYSWLL (p6.3). Futher investigation of the p6.2 and p6.3 peptides were not pursued due to their low presentation in selected phage population and high hydrophobicity.

Homology analysis of selected p6.1 peptide with known protein sequences.

The p6.1 peptide was analyzed for stretches of homology with known protein sequences from PIR (George et al., 1996) and SPTREMBL (Stoesser et al., 1999) protein sequence databases. The results of the FASTA sequence analysis (Pearson et al., 1988) for p6.1 are summarized in Table 2. We found that the six-amino acid p6.1 peptide shared a limited linear sequence homology with several different proteins (Table 2), including monocyte chemotactic protein (MCP), whey acidic protein (WAP), human spasmolytic protein (hSP), and the envelope protein of the Rous associated virus 1 (RAV1 Env). These proteins, each contained five-amino acid stretches of homology to p6.1 with 1 conservative substitution (CCYTL, KCCFS, KCCFS and CCFSL respectively). Of particular interest was the homology of p6.1 with hSP and RAV1 Env, since those proteins could be involved in direct interaction with ErbB receptors. Human SP belongs to the trefoil polypeptide family and has been implicated in the transient phosphorylation of ErbB-1 (Taupin et.al., 1999). The homology of p6.1 peptide with RAV1 Env could be indicative of functional significance, since ErbB-1 has been suggested as a possible receptor for several different viruses (Strong and Lee, 1996, Tang et al, 1993).

6

No linear sequence homology to p6.1 was found in any of the ErbB family ligands. However, the oxidized form of p6.1 could mimic a CC(Y/F) motif formed within the EGF-like domain of all known ErbB ligands due to C_{14}-C_{31} (EGF numbering) disulfide bond. Moreover, three of ErbB ligands, amphiregulin (AR), heregulin-α (HRG-α), and heregulin-$\beta 1$ (HRG-$\beta 1$), exhibit four-residue homology (KCCF) due to the presence of lysine residue next to the cysteine corresponding to C_{31} of the EGF.

Peptide synthesis and characterization

The p6.1 peptide and its biotinylated analog were chemically synthesized and purified to examine their binding activity in the absence of phage particle. Electrospray mass spectrometry was employed to confirm the molecular weight of the peptides and examine their conformations. Since the p6.1 sequence contained two cysteine residues, the peptide could exist in a reduced form, as an oxidized monomer, as a disulfide-bridged dimer or as a mixture. Figure 2A shows electrospray ionization mass spectrum (ESI-MS) of p6.1. The major peak corresponds to the ion [M*-H]⁻ at m/z 712 where M* is molecular weight of oxidized form of a single p6.1 molecule. There is also a peak at m/z 714, which we attribute to the reduced form of p6.1 [M-H]⁻. Figure 2B shows ESI-MS of biotinylated p6.1. There are two major peaks from the reduced p6.1 monomer ion [M*-H]⁻ at m/z 940 and from the oxidized p6.1 monomer [M-H]⁻ at m/z 938. These results suggest that the peptide exists in solution in two forms as an oxidized monomer and a reduced monomer. The mass spectrum method did not detect any presence of dimerized peptide in solution, which was consistent with the HPLC analysis. Since the molecules become protonated during the ionization procedure, we analyzed reduction conditions of the ESI technique on disulfide bond stability. For this purpose

7

we used commercially available oxidized glutathione, that exists as a disulfide-bonded peptide dimer (MW= 612). Mass spectrum of glutathione contained two major peaks from the ion [M-H]⁻ at m/z 611and from the [M-2H]²⁻ at m/z 305 (data not shown). There was no peak that corresponded to the reduced form of glutathione. Thus, the ESI procedure did not appear to reduce disulfide bridges and could be used for detection of the oxidized forms of the peptide.

Binding activity of p6.1 peptide

The binding specificity of synthetic p6.1 peptide to recombinant ErbB-2-ECD was examined by immunoblot and ELISA procedures. Immunoblot analysis was performed to compare the binding activity of the p6.1 peptide to ErbB-2-ECD and several other non-ErbB-2 related proteins. Purified recombinant ErbB-2-ECD as well as BSA, bovine asialofetuin, and human IgG were spotted on a nitrocellulose membrane at various amounts and exposed to the biotinylated p6.1 peptide. The p6.1 peptide bound only ErbB-2 and did not react with control proteins (Fig. 3A). Further ELISA analysis was performed to compare: first, binding activities of p6.1 and control peptide to ErbB-2-ECD and second, the binding activity of p6.1 to ErbB-2-ECD and to ErbB-1 receptor, which is a member of the same RTK family. Recombinant ErbB-2-ECD and ErbB-1 receptor from human carcinoma A431 cells were applied to plastic dishes and then incubated with the various concentrations of biotinylated p6.1 and a control peptide (biotin-RRLLFYKYVYKRYRAGKQRG). The p6.1 peptide demonstrated significant dose dependent binding activity to both ErbB-2-ECD and ErbB-1 protein, while the control peptide did not bind either ErbB-2-ECD or ErbB-1 (Fig 3B).

Fluorescence quenching experiments were performed in order to evaluate the equilibrium dissociation constant of p6.1 to the soluble Erb-2-ECD. Intrinsic tryptophan fluorescence of the protein was monitored as a function of peptide concentration. Since p6.1 peptide contains a tyrosine residue, samples were excited at 300 nm and monitored at 350 nm to minimize the influence of tyrosine emission on tryptophan fluorescence. Titration of ErbB-2-ECD with p6.1 resulted in substantial decrease of tryptophanyl fluorescence with maximum quenching of 20% under saturation conditions (data not shown). In our analysis we assumed a model with the stoichiometric ratio of protein to peptide equal to 1:1. The data were collected at 2μM, 4μM and 6μM concentrations of the protein. Theoretical curves were generated for the percentage of fluorescence quenching as a function of total peptide concentration (Fig. 3C). An apparent equilibrium dissociation constant, K_d = 30.2 +/- 7.6 μM, was determined using a nonlinear least-squares curve fitting procedure, which was applied to all three sets of data points obtained at different concentrations of protein with K_d as the shared constant for all curves.

Direct cell binding assay

We examined the ability of the p6.1 to recognize cultured human cancer cells expressing native conformation of the ErbB-2. High levels of ErbB-2 expression on DU-145 human prostate carcinoma cells has been reported previously (Zhau et.al., 1992). The MDA-MB-435 human breast carcinoma cells were shown to express moderate levels of the ErbB-2 protein (Hynes & Stern, 1994). In double immunostaining experiments both the anti-ErbB-2 mouse monoclonal antibody, and biotinylated p6.1 peptide bound prostate carcinoma cells DU-145 and MDA-MB-

435 cells (Fig. 4 B, C, E, and F). This result was consistent with experimental ELISA data (not shown) suggesting that the Neu (9G6) antibody used in our experiments and the p6.1 peptide do not compete for the same binding site on the extracellular domain of oncoprotein. The biotinylated control peptide (biotin-RRLLFYKYVYKRYRAGKQRG) did not bind DU-145 or MDA-MB-435 cells (data not shown). Neither the Neu (9G6) anti-ErbB-2 antibody, nor the biotinylated p6.1 bound T-24 human bladder carcinoma cells (Fig. 4 H, and I) used as negative control.

Discussion

ErbB-2 is a member of a family of growth factor receptors whose enhanced cellular is associated with tumor progression. New anti-cancer agents are being developed that directly bind tumor-associated determinants and thus are able to deliver drugs specifically to tumor cells. So far, there have been a few reports on identification of novel mAb (Masuko et.al., 1989; Yarden et.al., 1990; Baselga et al., 1998) and antibody fragments (Fab) (Clark et.al., 1997) that bind ErbB-2 receptor. Tumor targeting peptides offer an attractive alternative to antibodies and antibodies fragments due to their small size and *in vivo* pharmacokinetics. To our knowledge, this is the first report on identification of ErbB-2-binding peptide sequences using phage display technology. The synthetic peptide p6.1 selected from random 6-amino acid phage peptide library, exhibited specific binding activity to recombinant ErbB-2-ECD and to human cancer cells expressing ErbB-2 receptor. Remarkably, the disulfide constrained p6.1 peptide was derived from an unconstrained random peptide library. So far, only few unconstrained libraries have yielded putative disulfide constrained sequences (Devlin et al., 1990, Kay et al., 1993). Most of the reported disulfide-containing

peptides have been derived from libraries comprised of constrained peptides by design (Giebel et al., 1995, Oldenburg et al., 1992, Wrighton et al., 1996). In this study we have used the library with random amino acids peptide insert generated as a fusion near the N terminus of mature M13 viral pIII protein. There are eight cysteine residues in the mature pIII molecule. Since the phage particles are maintained in an oxidizing environment, one can reasonably suggest that two cysteines of the p6.1 insert could be disulfide-bonded not only with each other, but with the cysteines of the pIII protein as well. The latter, however, would likely interfere with the pIII structure resulting in a reduction of phage infectivity and underpresentation of the clone in the library. Thus, we believe that the cysteine residues of p6.1 displayed on the phage surface participate in disulfide bond formation within the peptide insert. Nevertheless, there is a possibility that the insert may exist in a reduced linear form on the surface of the phage.

Synthetic p6.1 exhibited binding activity not only to ErbB-2, but also to another member of the ErbB receptor family, ErbB-1. This result was not surprising, since there is an overall 40-50% homology between ErbB-2 and ErbB-1. We suggest that the binding activity of p6.1 peptide toward both ErbB-2 and ErbB-1 is related to its constrained nature. The oxidized form of p6.1 (Fig. 5B) could mimic a CC(Y/F) motif, found in the structure of the EGF-like domain of all known ErbB ligands (Fig. 5C). The CC(Y/F) motif is formed due to the C_{14}-C_{31} (EGF numbering) disulfide bridge (Fig. 5A). The residues participating in the formation of this motif, two cysteines and a semi-conservative aromatic amino acid (Y/F), are invariant in all of the ErbB family ligands (Fig. 5C). Such invariance suggests the importance of these amino acids in defining either a structure or the binding properties of the EGF-like proteins. Phenylalanine from the CCF motif of TGF-α was shown to appear on its binding interface (McInnes & Sykes, 1997). Remarkably,

11

another EGF-like polypeptide, Cripto-1, which is not known to bind any of the ErbB receptors, does not contain CCY/F motif in its structure.

The ability of the synthetic p6.1 to recognize the native conformation of ErbB-2 was examined in direct cell binding assays with human cancer cell lines known to express different levels of the receptor. As revealed by fluorescent microscopy, the biotinylated p6.1 peptide bound DU-145 human prostate carcinoma and MDA-MB-435 human breast carcinoma cells, but did not bind T-24 human bladder carcinoma cells. The overall levels of the binding of the peptide to target cells were in agreement with the levels of ErbB-2 expression reported for the cell lines used. However, in double immunostaining experiments, we noticed some differences in the patterns of cell-to-cell distribution of the anti-ErbB-2 antibodies and synthetic p6.1. We attributed these differences to the ability of the p6.1 peptide to bind the ErbB-1 as well.

These studies demonstrate that the p6.1 peptide is able to bind recombinant ErbB-2-ECD and ErbB-1 receptor from human carcinoma cells. Moreover, the p6.1 is capable to distinguish tumor cells overexpressing ErbB-2 receptor from those cells, which have low expression of ErbB-2. In conclusion, the peptide KCCYSL has the potential to be developed into a cancer imaging or therapeutic agent targeting malignant cells overexpressing ErbB-2 receptor.

Materials and Methods

Cell culture and maintenance

The HEK-293 human embryonic kidney cells, as well as DU-145 human prostate carcinoma, and T-24 human bladder carcinoma cell lines were purchased from ATCC. The MDA-MB-435 human

breast carcinoma cell line was kindly provided by Dr. Janet E. Price, M.D. Anderson Cancer Center, Houston, TX. All cells were maintained as monolayer cultures in either DMEM (HEK-293 human embryonic kidney cells) or RPMI-1640 (DU-145 human prostate carcinoma, MDA-MB-435 human breast carcinoma, and T-24 human bladder carcinoma cells) medium supplemented with 10% fetal bovine serum (FBS), sodium pyruvate, nonessential amino acids, and L-glutamine. The cultures were maintained at 37°C in a 5% CO_2 humidified incubator. Subculturing was performed using standard trypsinization procedures.

Expression and purification of ErbB-2-ECD

The eukaryotic expression plasmid c-erbB-2-pRc/CMV$_{FLAG}$ encoding ErbB-2-ECD tagged with a FLAG epitope at C-terminus was used to create a cell line stable expressing the FLAG-tagged ErbB2-ECD fusion protein (Clark et.al., 1997). The human embryonic kidney cells HEK-293 were transfected with 20 μg of recombinant DNA using a calcium phosphate precipitation kit (Stratagene) in accordance to manufacturer's protocol. Stable transfectants were selected in medium (DMEM + 10% FBS) containing G418 (0.5 mg/ml). Individual clones arising from single cells were isolated using 8x10 cloning cylinders (Sigma). The supernatant from each clone was assayed for the expression of recombinant protein by Western blot and ELISA using Neu (9G6) anti-ErbB-2 mouse monoclonal antibody (Santa Cruz Biotechnology). The highest expressing clone was chosen for future experiments.

The filtered supernatant taken from HEK293 cells that secreted ErbB-2-ECD into the medium, was run on anti-FLAG M2 affinity column equilibrated with 20 mM Tris (pH=8.0), 150 mM NaCl. Bound protein was eluted with 0.1 M glycine (pH=3.0) and neutralized with 1M Tris HCl (pH=8.0).

13

The protein was concentrated and dialyzed against PBS, and NaN$_3$ was added to prevent bacterial growth.

Western blot analysis of ErbB-2-ECD

Purified ErbB-2-ECD was subjected to SDS-polyacrylamide gel electrophoresis (Laemmli, 1970), and transferred to a nitrocellulose filter. The filter was subsequently blocked with 1% BSA in PBS (pH=7.4), and exposed to Neu(9G6) anti-ErbB-2 mouse monoclonal antibody. The bound antibody was detected by anti-mouse secondary antibody coupled to alkaline phosphatase. Color reaction was performed using 5-bromo-4-chloro-3indonyl phosphate (BCIP) and nitro blue tetrazolium (NBT).

Size-exclusion HPLC analysis

Size-exclusion chromatography was performed on a BIOPSEP SEC-S2000 column equilibrated with 0.05 M phosphate buffer pH=6.8. A flow rate of 0.5 ml/min was maintained throughout the experiments. The elution volume of dextran served as void volume. Trypsin inhibitor, chicken egg albumin, human albumin, and mouse IgG served as molecular weight markers. Recombinant ErbB-2-ECD (10 μg) was used to inject the column. The elution volume for each injected protein was measured as a function of protein molecular weight.

Affinity selection

The affinity selection was performed following a protocol described by G. Smith on the website http:/www.biosci.missouri.edu/SmithGP (Smith & Scott, 1993). Briefly, wells of the microtiter

plates were first coated with streptavidin, washed with TPBS (phosphate buffered saline, pH 7.4, 0.5% (v/v) Tween-20), and then blocked with 3% (w/v) BSA. Biotinylated antigen was incubated with streptavidin coated plates for 2 hours at 4° C. In first and second round of selection 10 μg of biotinylated antigen per plate was added, in third round amount of antigen was decreased to 1 μg, and for fourth round of selection 0.1 μg of antigen was used. Unoccupied biotin-binding sites were blocked with 0.1 mM biotin. Phage was incubated with antigen for 4 hours at RT. Plates were washed 10 times with TPBS to remove unbound phage. Bound phage was eluted with elution buffer (0.1 M HCl, pH is adjusted to 2.2 with glycine, 1mg/ml BSA, 0.1mg/ml phenol red) at RT during 10 min. The increased percentage of bound phage to input phage (yield) was an intrinsic characteristic of successful biopanning. After each round, except the last, the eluate of the bound phage was propagated and used as input for the next round. Individual clones were characterized by DNA sequencing after the fourth round of selection.

DNA sequencing analysis

Individual phage isolates were sequenced manually by a modified dideoxy sequencing methodology as described by G. Smith on the website http:/www.biosci.missouri.edu/SmithGP (Haas & Smith, 1993).

Sequence comparison

The sequence homology searches were performed using the FASTA program of the University of Wisconsin Genetics Computer Group program package (GCG, version 10.0-Unix, January 1999). EMBL and PIR-protein databases were released 3/97 and 6/99 respectively.

Peptide synthesis

The peptides were chemically synthesized on the Applied Biosystems peptide synthesizer 431A using FMOC-based chemistry.

Mass spectrometric analysis

Mass Consortium Corporation, San Diego, performed the mass spectrometric analysis. Commercially available oxidized form of gluthatione (Sigma # G4501) was used as control for reduction conditions.

Immunoblot analysis of binding activity of the p6.1 peptide

ErbB-2-ECD and three other proteins, bovine serum albumin (BSA, Sigma #A-3912), asialofetuin (AF, Sigma #A-4781), and human IgG (Sigma #I-2511) were immobilized on a nitrocellulose membrane at various quantities (6.25 – 50 ng) and then incubated with 1% blocking reagent (Boehringer Mannheim, cat # 1096 176) in phosphate buffered saline (PBS) pH=7.4. After washing three times with PBS, the membrane was incubated with 100μM biotinylated peptide for 2 hours at RT. The membrane was washed and incubated with alkaline phosphatase labeled streptavidin (Sigma #S-2890) for 1 hour RT. The staining reaction was performed using 50 μl NBT

and 37.5 µl X-phosphate solutions (Boehringer mannheim, cat # 1383 213) in 10 ml 0.1M Tris buffer, pH=9.5, 0.05 M MgCl, 0.1 M NaCl.

ELISA

100 ng of ErbB-2-ECD or ErbB-1 (Sigma # E-2645) in PBS was applied to polystyrene wells (Costar #3590) overnight at +4° C. Coated wells were washed three times with TPBS (phosphate buffered saline, pH 7.4, 0.5% (v/v) Tween-20) and blocked with 1% blocking reagent (Boehringer Mannheim # 1096 176) in PBS for 1 h at RT. Wells were subsequently incubated with biotinylated peptide added to the wells by serial dilutions (1:2) at RT for 2 h. After washing three times with TPBS, wells were incubated with alkaline phosphatase labeled streptavidin (Sigma # S-2890) for 1 h at RT. Bound alkaline phosphotase was developed using 1 mg/ml p-Nitrophenyl Disodium Phosphate (Sigma # N-9389) in 1M diethanolamine buffer, 0.5 mM $MgCl_2$, pH=9.8. The pNPP reaction was stopped with 3M NaOH. Optical density was measured at 405nm in a microplate reader. All assays were performed at least three times in triplicate wells. Values are reported as an average of absorbence +/- SD.

Cell binding assay

DU-145 (human prostate adenocarcinoma), MDA-MB-435 (human breast carcinoma), and T-24 (human bladder carcinoma) cells were grown directly on the same microscope slide using a 4 well Lab-Tek II chamber slide system (Nalge Nunc). When cultures reached approximately 60-70 % confluence, the cells were briefly washed with PBS, fixed with 4% formaldehyde solution in PBS for 30 minutes but not permeabilized, and preblocked for 1 hr with 2% bovine serum albumin

(BSA) solution in PBS at 37°C. The cultivation chambers were removed and cells were incubated for 2 hr with solution of Neu (9G6) anti-ErbB-2 mouse monoclonal antibody (Santa Cruz Biotechnology) diluted 1:100 and biotinylated peptide (100μM) in 2% solution BSA in PBS. The slides were washed three times with PBS followed by 1 hr incubation with Lissamine Rhodamine-conjugated donkey anti-mouse IgG (Jackson ImmunoResearch Laboratories) and streptavidin-AMCA-S conjugate (Molecular Probes) in 2% BSA in PBS. After additional washes with PBS, the slides were mounted and analyzed by fluorescent microscopy using Rhodamine and UVA filter sets.

Fluorescence assay

The fluorescence titration experiments were carried out using a SLM Aminco spectrofluorometer interfaced to a DEL 433/L PC running SLM Aminco 8100 series 2 software. The titrations were performed at 25°C with varying amounts of peptide added to a fixed ErbB-2-ECD concentration (200 – 600 nM) in 2 ml of phosphate buffered saline (pH=7.4). Each measurement was collected for 5-20 sec after 1-2 min pre-equilibration. The excitation shutter remained closed during pre-equilibration of the sample and was opened only during data acquisition in order to minimize photobleaching of the sample. The fluorescence measurements were corrected for dilutions and photobleaching of ErbB-2-ECD. Values reported are an average of three independent measurements. We neglected the difference between total peptide concentration and free peptide concentration since the concentration of the peptide was much higher than concentration of the protein during the entire experiment. The fitting procedure was performed using Origin (Microcal Software Inc).

Acknowledgments

References

Ballinger, M.D., Jones, J.T., Lofgren, J.A., Fairbrother, W.J., Akita, R.W., Sliwkowski, M.X., Wells, J.A. (1998). Selection of heregulin variants having higher affinity for the ErbB3 receptor by monovalent phage display. *J. Biol. Chem.* **273:19**, 11675-84.

Baselga, J., Norton, L., Albanell, J., Kim, Y-M., & Mendelson, J. (1998) Recombinant humanized anti-HER2 antibody (Herceptin) enhances the antitumor activity of paclitaxel and doxorubicin against HER2/*neu* overexpressing human breast cancer xenografts. *Cancer Res.* **58,** 2825-2831.

Clark, M.A., Hawkins, N.J., Papaionnou, A., Fiddes, R.J., Ward, R.L. (1997). Isolation of human anti-c-erbB-2 Fabs from a lymph node-derived phage display library. *Clin. Exp. Immunol.* **109**, 166-174.

De Potter, C.R., Daele, S.V., Van De Vijver, M.J., Pauwels, C., Maertens, G., De Boever, J., Vanderkerckhove, D., Roels, H. (1989). The expression of the neu oncogene product in breast lesions and in normal fetal and adult human tissues. *Histopathol.* **15**, 351-362

Devlin, J.J., Panganiban, L.C., Devlin, P.E. (1990). Random peptide libraries: a source of specific

protein binding molecules. *Science,* **249**, 404-6.

Disis, M.L., Grabstein, K.H., Sleath, P.R., Cheever, M.A. (1999). Generation of immunity to the HER2/neu oncogenic protein in patients with breast and ovarian cancer using a peptide-based vaccine. *Clin. Cancer Res.*, **5:6**, 1289-97.

Doorbar, J. and Winter, G. (1994). Isolation of a peptide antagonist to the trombin receptor using phage display. *J. Mol.Biol.*, **244:4**, 361-9.

Fischman, A.J., Babich, J.W. and Strauss, H.W. (1993). A ticket to ride: peptide radiopharmaceuticals. *J. Nucl. Med.*, **34:12**, 2253-63.

George, D.G., Barker, W.C., Mewes, H.W., Pfeiffer, F. and Tsigita, A. (1996). The PIR international protein sequence database. *Nucl. Acids Res.*, **24**, 17-20.

Giebel, L.B., Cass, R.T., Milligan, D.L., Young, D.C., Arze, R., Johnson C.R. (1995). Screening of cyclic peptide phage libraries identifies ligands that bind streptavidin with high affinities. *Biochemistry,* **34**, 15430-35.

Haas, S.L. and Smith, G.P. (1993). Rapid screening of viral DNA from filamentous bacteriophage. *Biotechniques,* **15**, 422-424.

Harris, J.D., Gutierrez, A.A., Hurst, H.C., Sikora, K., Lemoine, N.R. Gene therapy for cancer using tumour-specific prodrug activation. *Gene Ther.*, **1:3**, 170-5.

Hynes, N.E. & Stern, D.F. (1994). The biology of *erbB-2/neu/HER-2* and its role in cancer. *Biochim. Biophys. Acta,* **1198**, 165-184.

Jinno, H., Ueda M., Enomoto, K., Ikeda, T., Kyriakos, P., Kitajima, M. (1996). Effectiveness of an adriamycin immunoconjugate that recognizes the C-erbB-2 product on breast cancer cell lines. *Surg. Today,* **26:7**, 501-7.

Jones, J.T., Akita, R.W., and Sliwkowski, M.X. (1999). Binding specificities and affinities of *egf* dpmains for ErbB receptors. *FEBS Letters,* **447**, 227-231.

Jones, J.T., Ballinger, M.D., Pisacane, P.I., Lofgren, J.A., Fitzpatrick, V.D., Fairbrother, W.J., Wells, J.A., and Sliwkowski, M.X. (1998). Binding interaction of heregulinβ *egf* domain with ErbB3 and ErbB4 receptors assessed by alanine scanning mutagenesis. *The J. Biol. Chem.,* **273:19**, 11667-11674.

Kay, B.K., Adey, N.B., He, Y.S., Manfredi, J.P., Mataragnon, A.H., Fowlkes, D.M. (1993). An M13 phage library displaying random 38-amino-acid peptides as a source of novel sequences with affinity to selected targets. *Gene,* **128**, 59-65.

Laemmli, U.K. (1970). Cleavage of structural proteins during the assembly of the head of bacteriophage T4. *Nature*, **227**, 680.

Lee, K-F., Simon, H., Chen, H., Bates, B., Hung, M-C., Hauser, C. (1995). Requirement for neuregulin receptor erbB2 in neural and cardiac development. *Nature,* **378**, 394-97.

Masuko, T., Sugahara, K., Kozono, M., Otsuki, S., Akiyama, T., Yamamoto, T., Toyoshima, K., and Hashimoto, Y. (1989). A murine monoclonol antibody that recognizes an extracellular domain of the human *c-erbB-2* protooncogene product. *Jpn. J. Cancer Res.,* **80**, 10 – 14.

McInnes, C. & Sykes, B.D. (1997). Growth factor receptors: structure, mechanism, and drug discovery. *Biopolymers,* **43:5**, 339-66.

Murayama O., Nishida H., Sekiguchi K. Novel peptide ligands for integrin alpha 6 beta1 selected from a phage display library. *J. Biochem. (Tokyo)*, **120:2**, 445-51.

Oldenburg, K.R., Loganathan, D., Goldstein, I.J., Schultz, P.G., Gallop, M.A. (1992). Peptide ligands for a sugar-binding protein isolated from a random peptide library.

Proc. Natl. Acad. Sci., **89**, 5393-97.

Pearson, W.R. and Lipman, D.J. (1988). Improved tools for biological sequence comparison.

Proc. Natl. Acad. Sci., **85:8**, 2444-8.

Peles E. and Yarden Y. (1993). Neu and its ligands: from an oncogene to neural factors. *BioEssays,*

15:12, 815-24.

Peletskaya, E.N., Glynsky, V.V., Glinsky, G.V., Deutscher, S.L., and Quinn, T.P. (1997).

Characterization of peptides that bind the tumor-associated Thomsen-Friedenreich antigen

selected from bacteriophage display libraries. *J. Mol. Biol.,* **270**, 374-384.

Peletskaya, E.N., Glinsky, G.V., Deutscher, S.L., and Quinn, T.P. (1996). Identification of peptide

sequences that the Thomsen-Friedenreich cancer-associated glycoantigen from

bacteriophage peptide display libraries. *Mol. Diversity,* **2**, 13-18.

Piccart, M.J., Awada, A., & Hamilton, A. (1999) in American Society of Clinical

Oncology Educational Book, Perry,M.C.:Editor. 1999 American Society of

Clinical Oncology, Alexandria, VA.

Renschler, M.F., Wada, H.G., Fok, K.S., Levy, R. (1995). B-lymphoma cells are activated by

peptide ligands of the antigen bindingreceptor or by anti0idiotypic antibody to induce

extracellular acidification. *Cancer Res.,* **55:23**, 5642-7.

Scott, J.K., Smith, G.P. (1990). Searching for peptide ligands with an epitope library. *Science,* **249**,

386-90.

Shelly, M., Pinkas-Kramarski, R., Guarino, B.C., Waterman, H., Wang, L.M., Lyass, L., Alimandi,

M., Kuo, A., Bacus, S.S., Pierce, J.H., Andrews, G.C., and Yarden, Y. (1998) Epiregulin is

a potent pan-ErbB ligand that preferentially activates heterodimeric receptor complexes. *J.*

Biol. Chem., **273:17,** 10496-10505.

Smith, G.P., Scott, J.K. (1993). Libraries of proteins and peptides displayed on filamentous phage. *Methods Enzymol.,* **217,** 228-257.

Stoesser, G., Tuli, M.A., Lopez, R., Sterk P. (1999). The EMBL Nucleotide Sequence Database. *Nucl. Acids Res.,* **27:1,** 18-24.

Strong, J.E., & Lee, P.W. (1996) The v-erbB oncogene confers enhanced cellular susceptibility to retrovirus infection. *J. Virol.* **70,** 612-616.

Taupin, D., Deng-Chyang Wu, Woo-Kyu Jeon, Devaney, K., Wang, T.C., & Podolsky, D.K. (1999) The trefoil gene family are coordinately expressed immediate-early genes: EGF receptor- and MAP kinase-dependent interregulation. *J. Clin. Invest.* **103,** R31-R38.

Vennstrom, B., Raynoscheck, C., Jansson, L., Doederlein, G., Lhotak, V., Johnsson, A., Beug, H. (1994). Retroviral capture of c-*erb*B proto-oncogene sequences: rapid evolution of distinct viral genomes carrying mutant v-*erb*B genes with different transforming capacities. *Oncogene,* **9:5,** 1305-20.

Walker, K., Perkins, M., Dray, A. (1995). Kinins and kinin receptors in the nervous system. *Neurochem. Intt.,* **26:1** 1-16.

Weiner, L.M., Clark, J.I., Davey, M., Li, W.S., Garcia de Palazzo I., Ring, D.B., Alpaugh, R.K. (1995). Phase I trial of 2B1, bispecific monoclonal antibody targeting c-erbB-2 and Fc gamma RIII. *Cancer Res.,* **55:20,** 4586-93.

Wienchen, K. and Dietel M. (1995). C-erbB-2 antisense phosphorothioate oligodeoxynucleotides inhibit growth and serum-induced cell spreading of P185 c-erbB-2 overexpressing ovarian carcinoma cells. *Int. J. Cancer,* **63:4,** 604-8.

Wrighton, N.C., Farrel, F.X., Chang, R., Kashyap, A.K., Barbone, F.P., *et.al.* (1996). Small peptides

as potent mimetics of the protein hormone erythropoitin. *Science,* **273**, 458-63.

Wu, J.T., Astill, M.E., Zhang, P. (1993). Detection of the extracellular domain of c-erbB-2

oncoprotein in sera from patients with various carcinomas: correlation with tumor markers.

J. Clin. Lab. Anal. **7**, 31-40.

Yarden, Y. (1990). Agonistic antibodies stimulate the kinase encoded by the neu protooncogene in

living cells but the oncogenic mutant is constitutively active. *Proc. Natl. Acad. Sci. U.S.A.*

87, 259-2573

Zhau, H.E., Wan, D.S., Zhou, J., Miller, G.J., and von Eschenbach, A.C. (1992). Expression of c-

erb B-2/neu proto-oncogene in human prostatic cancer tissues and cell lines. *Mol.*

Carcinogenesis. **5:4**, 320-327.

Table 1. Affinity selected peptide sequences

Name	Peptide Sequence	Library	% Of Clones*
p6.1	KCCYSL	F3-6	75
p6.2	WYAWML	F3-6	8
p6.3	WYSWLL	F3-6	10

*The percent of individual clones that were represented in the affinity selected and sequenced phage clones.

Table 2. Homology of p6.1 peptide with known protein sequences

Name	Sequence	Position
p6.1	KCCYSL	
Monocyte Chemotactic Protein, Bovine	CCYTL	9-13[**]
Whey Acidic Protein, Camel	KCCFS	97-101[**]
Spasmolytic Protein, Human	KCCFS	106-110[**]
Envelope Protein, Rous Associated Virus 1	CCFSL	9-13[*]

[a]*Bold,* invariant amino acids; *regular,* equivalent amino acids.
[*]Amino acid numbers derived from the sequences deposited in STREMBL data bank.
[**]Amino acid numbers derived from the sequences deposited in PIR data bank.

Figure legends

Figure 1. Western blot analysis of the anti-FLAG affinity purified recombinant human ErbB-2-ECD. Molecular weight markers (MWM) and their associated values are given on the left.

Figure 2. The ES-MS analysis of synthetic p6.1 peptide (A), and biotinylated synthetic p6.1 (B). *Arrows,* major peaks corresponding to molecular mass of the oxidized p6.1 monomer (712), reduced p6.1 monomer (714), oxidized biotinylated p6.1 monomer (938), and reduced biotinylated p6.1 monomer (940)
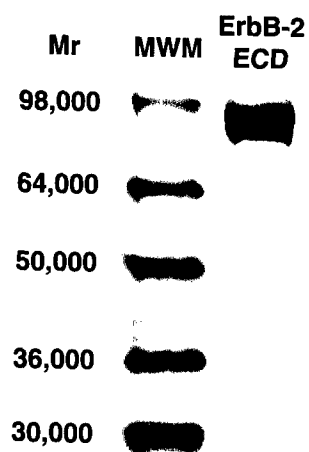

Figure 3. A, immunoblot analysis of the binding activity of biotinylated synthetic p6.1 peptide (100μM) to the recombinant human ErbB-2-ECD, bovine serum albumin (BSA), bovine asialofetuin (ASF), and human IgG. The quantities of immobilized proteins (in ng) are given on the top. B, binding profiles of biotinylated p6.1 and biotinylated control peptide (CP) to immobilized recombinant ErbB-2-ECD (▼——▼ p6.1, +——+ CP), and ErbB-1 (♦——♦ p6.1, ×——× CP). C, fluorescent titration of the ErbB-2-ECD with synthetic p6.1 peptide at 0.2 μM protein (■), 0.4 μM protein (●), and 0.6 μM protein (▲).

Figure 4. Direct cell binding of Neu(9G6) anti-ErbB-2 mouse monoclonal antibody and biotinylated p6.1 peptide to DU-145 human prostate carcinoma (top panel), MDA-MB-435 human breast carcinoma (middle panel), and T-24 human bladder carcinoma (bottom panel) cells. In
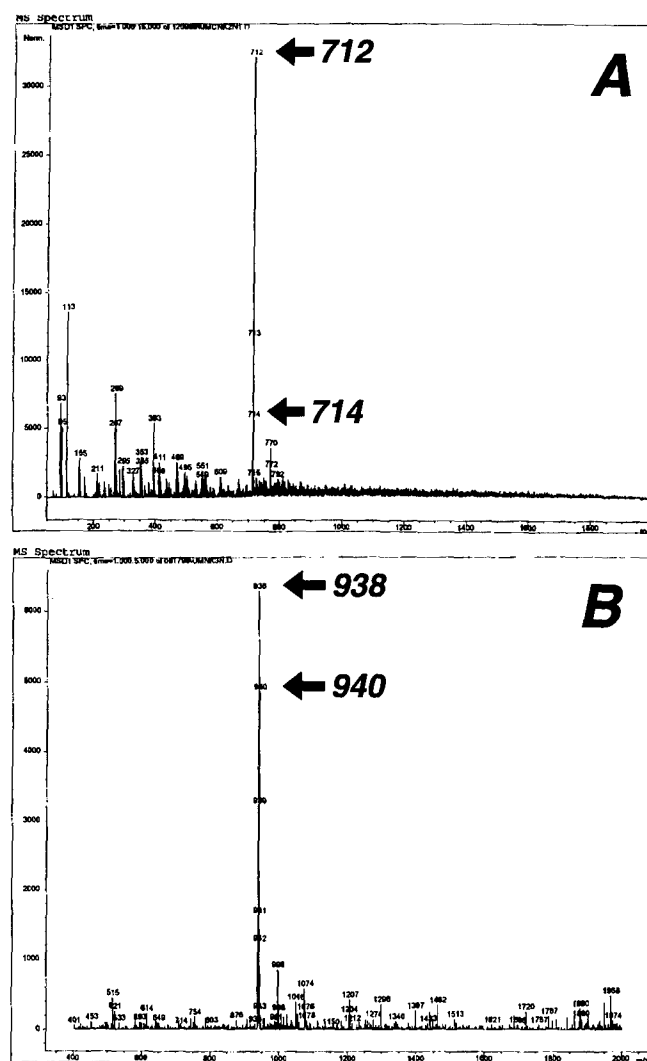
double immunostaining experiments both Neu(9G6) anti-ErbB-2 antibody (B and E) and

biotinylated p6.1 (C and F) bound DU-145 and MDA-MB-435 cells expressing high and moderate

levels of ErbB-2 protein, respectively. Neither the Neu(9G6) antibody (H) nor the p6.1 peptide (I)

bound T-24 bladder carcinoma cells used as control. Panel A, D, and G are phase contrast

photomicrographs of the respective fields.

Figure 5. A, Schematic presentation of the EGF primary structure arranged to demonstrate the

formation of CCY motif due to C_{14}-C_{31} disulfide bond. Red letter K next to N_{32} indicates the lysine

corresponding to K_{71} of AR, and K_{111} of HRG-α and HRG-β. B, backbone structure of oxidized

form of p6.1 peptide. C, sequence alignment of the amino acids 13-32 fragment of EGF with

corresponding fragments of several other ErbB ligands. The amino acid residues participating in

formation of KCCY/F motif colored in red. *Arrows,* indicate a direction of the KCCY/F motif.
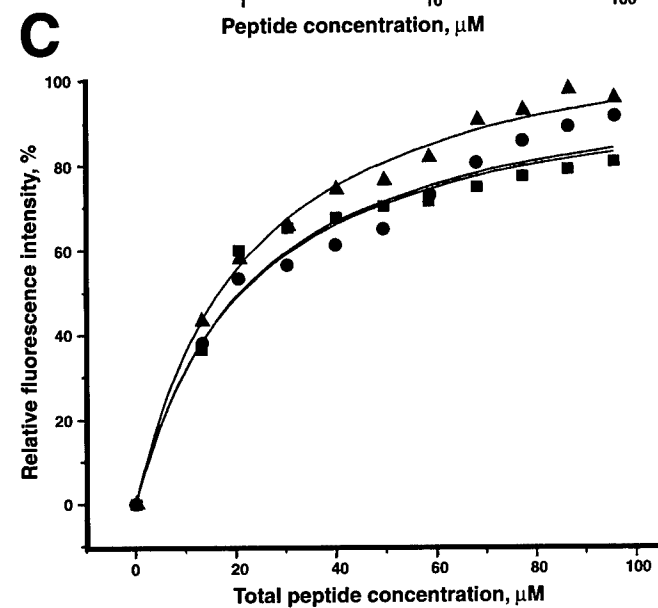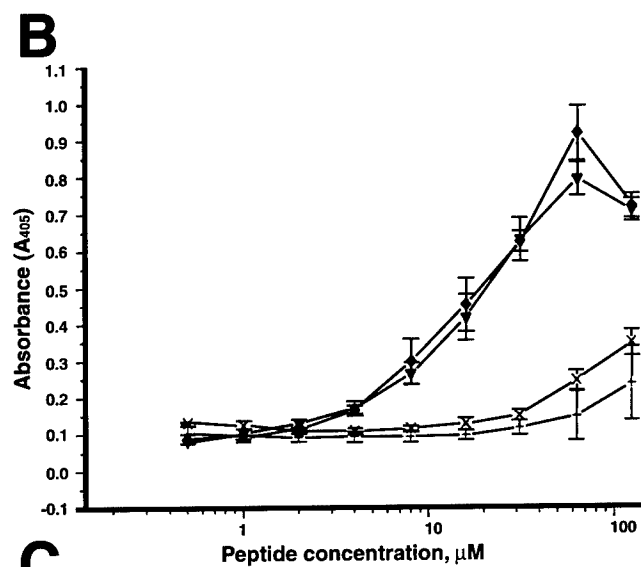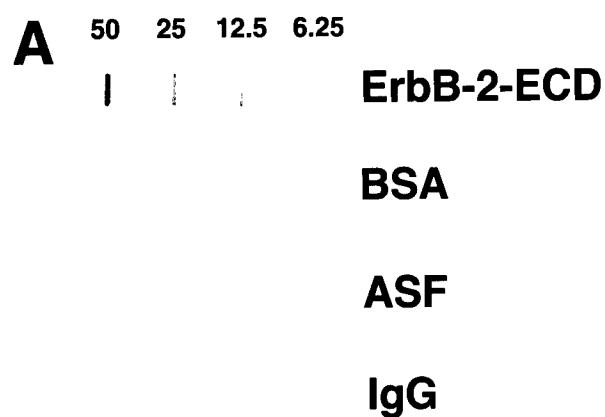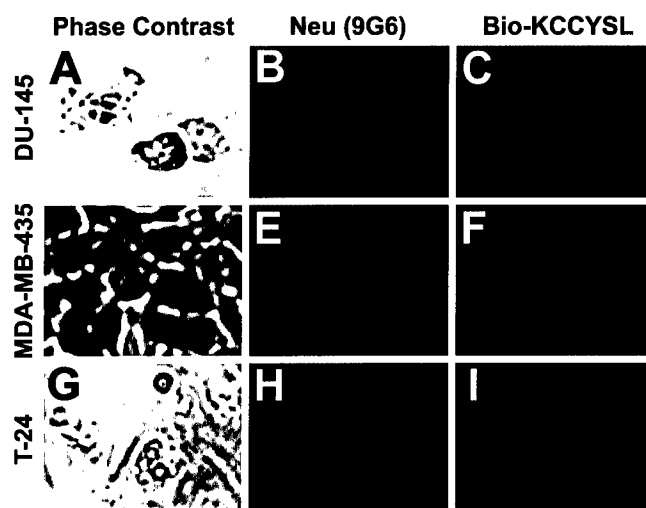
FIGURE 1

	Mr	MWM	ErbB-2 ECD
	98,000		
	64,000		
	50,000		
	36,000		
	30,000		

FIGURE 2

A

←712

←714

B

←938

←940

FIGURE 3

A

50   25   12.5   6.25

ErbB-2-ECD

BSA

ASF

IgG

B

Y-axis: Absorbance (A₄₀₅) — $Absorbance\ (A_{405})$ — 1.1, 1.0, 0.9, 0.8, 0.7, 0.6, 0.5, 0.4, 0.3, 0.2, 0.1, 0.0, -0.1

X-axis: Peptide concentration, µM — 1, 10, 100

C

Y-axis: Relative fluorescence intensity, % — 0, 20, 40, 60, 80, 100

X-axis: Total peptide concentration, µM — 0, 20, 40, 60, 80, 100

FIGURE 4

	Phase Contrast	Neu (9G6)	Bio-KCCYSL
DU-145	A	B	C
MDA-MB-435	D	E	F
T-24	G	H	I

FIGURE 5

A

B

K C C Y S L

C

EGF	YCLHDGVCMY I EALD---KYACN	
TGF-α	FCFH-GTCRF LVQED---KPACV	
AR	FC I H-GECKY I EHLE---AVTCK	
HB-EGF	FC I H-GECKYVKELR---APSC I	
BC	YC I H-GRCRF VVDEQ---TPSC I	
HRG-α	FCVNGGEC FMVKDLSNPSRYLCK	
HRG-β	FCVNGGEC FMVKDLSNPSRYLCK	

Advances in Brief
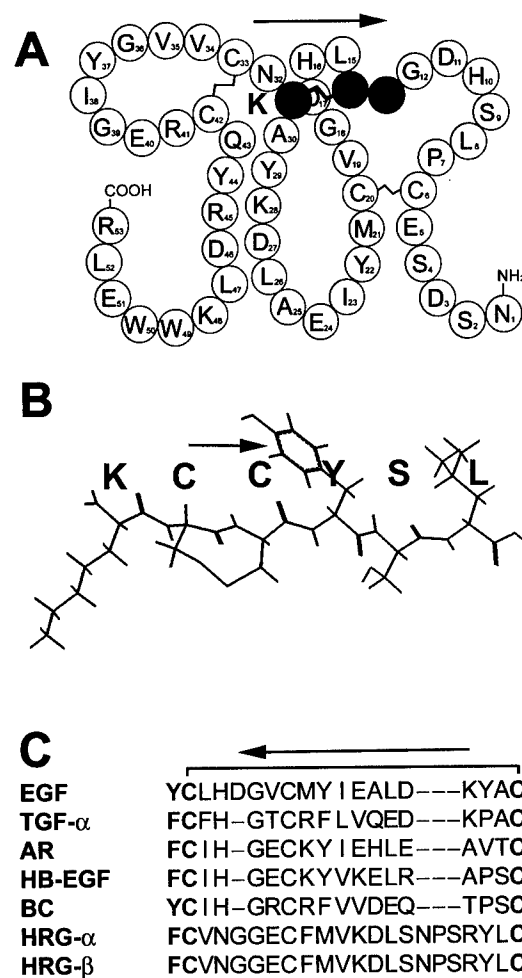
Effects of Thomsen-Friedenreich Antigen-specific Peptide P-30 on β-Galactoside-mediated Homotypic Aggregation and Adhesion to the Endothelium of MDA-MB-435 Human Breast Carcinoma Cells[1]

Vladislav V. Glinsky, Margaret E. Huflejt, Gennadi V. Glinsky, Susan L. Deutscher, and Thomas P. Quinn[2]

Cancer Research Center [V. V. G.] and Department of Biochemistry [V. V. G., S. L. D., T. P. Q.], University of Missouri, Columbia, Missouri 65211; La Jolla Institute for Allergy and Immunology [M. E. H.], San Diego, California 92121; and Sidney Kimmel Cancer Center and Metastat, Inc. [G. V. G.], San Diego, California 92121

Abstract

Both the ability of malignant cells to form multicellular aggregates via homotypic or heterotypic aggregation and their adhesion to the endothelium are important if not critical during early stages of cancer metastasis. The tumor-associated carbohydrate Thomsen-Friedenreich antigen (T antigen) and β-galactoside binding lectins (galectins) have been implicated in tumor cell adhesion and tissue invasion. In this study, we demonstrate the involvement of T antigen in both homotypic aggregation of MDA-MB-435 human breast carcinoma cells and their adhesion to the endothelium. The T antigen-specific peptide P-30 (HGRFILPWWYAFSPS) selected from a bacteriophage display library was able to inhibit spontaneous homotypic aggregation of MDA-MB-435 cells up to 74% in a dose-dependent manner. Because T antigen has β-galactose as a terminal sugar, the expression profile of β-galactoside-binding lectins (galectins) in MDA-MB-435 cells was studied. Our data indicated the abundant expression of [^{35}S]methionine/cysteine-labeled galectin-1 and galectin-3 in this cell line, which suggested possible interactions between galectins and T antigen. As revealed by laser confocal microscopy, both galectin-1 and galectin-3 also participate in the adhesion of the MDA-MB-435 cells to the endothelium. We observed the clustering of galectin-3 on endothelial cells at the sites of the contact with tumor cells, consistent with its possible interaction with T antigen on cancer cells. The galectin-1 signal, however, strongly accumulated at the sites of cell-cell contacts predominantly on tumor cells. The T antigen-specific P-30 significantly (50%) inhibited this adhesion, which indicated that T antigen participates in the adhesion of MDA-MB-435 breast cancer cells to the endothelium. The ability of synthetic P-30 to inhibit both the spontaneous homotypic aggregation of MDA-MB-435 cells and their adhesion to the endothelium (>70 and 50%, respectively) suggests its potential functional significance for antiadhesive therapy of cancer metastasis.

Introduction

Understanding the molecular underpinnings of cancer metastasis is an important goal of modern cancer research. Metastasis is a multistep process involving many cell-cell and cell-extracellular matrix interactions. Several of these steps include interactions between cell surface molecules such as carbohydrates, lectins, and extracellular matrix proteins participating in cell-cell recognition and adhesion (1, 2). Whereas the initial steps of metastasis include detachment of malignant cells from the primary tumor and migration into the circulatory system, subsequent steps involve malignant cells adhering to each other (homotypic aggregation) or to host cells (heterotypic adhesion;

Refs. 3–6) to form multicellular aggregates. Eventually, the circulating tumor cells bind to capillary endothelial cells and to exposed basement membrane proteins, which results in the formation of secondary tumor sites. Recent observations by Al-Mehdi *et al.* (7) indicate the critical role of adhesion of the cancer cells to the vascular endothelium in this process. They demonstrated that only endothelium-attached rather than extravasated cancer cells are capable of giving rise to hematogenous cancer metastases (7). It has been suggested that tumor cell adhesion is, in part, mediated by specific interactions between cell surface lectins and carbohydrates present on glycoproteins, glycolipids, and glycosaminoglycans (2, 4, 8, 9).

There has been a tremendous surge in research to characterize the roles of cell surface carbohydrate structures in cell-cell communication as mediators of tumor cell proliferation, adhesion, and metastasis. Alterations in cell surface carbohydrate structures of cancer cells are postulated to effect normal cellular interactions and have been shown to facilitate tumor cell colonization and metastasis (2, 3, 8). One such cancer-associated carbohydrate antigen, the T antigen,[3] has been the focus of much research into its role in tumor cell adhesion and metastasis (8). The immunodominant portion of the T antigen is the terminal Galβ1 → 3GalNAc carbohydrate moiety (5). Cryptic, covalently or structurally masked and nonimmunoreactive, T antigen is present on the surfaces of healthy cells in most tissues. It is, however, exposed and immunoreactive on most human carcinomas and T-cell lymphomas (8, 10). T antigen has been proposed to be involved in tumor cell adhesion and tissue invasion. The existence of T antigen-mediated cell adhesion between highly metastatic murine lymphoma cells and hepatocytes is supportive of a role for this cell surface carbohydrate structure in the metastatic process (6). Large quantities of T antigen have been detected on the outer surface membranes of human breast carcinomas, which makes it an attractive target for the development of tumor diagnostic and therapeutic agents (10, 11). In our laboratory, several peptides that bind T antigen have been affinity-selected from a 15-amino-acid-random-peptide bacteriophage display library and characterized for their binding affinities and specificities (12, 13). One of the peptides, P-30, has been shown to selectively bind several cancer cell lines that display T antigen on their surfaces including MDA-MB-435 human breast carcinoma cells. It was also found to efficiently inhibit asialofetuin-induced homotypic aggregation of B16-F1 murine melanoma cells (13). We hypothesized that if T antigen mediates spontaneous homotypic aggregation of breast cancer cells, then a T antigen-binding peptide may likewise inhibit this aggregation. In this study, we demonstrate that T antigen accumulates at the sites of cell contact in multicellular aggregates of MDA-MB-435 human breast carcinoma cells, which suggests the

---

involvement of T antigen in spontaneous aggregation. Indicative of the participation of T antigen in homotypic aggregation is the ability of T antigen-specific P-30 to significantly (>70%) inhibit this aggregation in a dose-dependent manner.

Cell type-specific carbohydrates facilitate cell-cell communication through selective interactions with carbohydrate-binding proteins, including cell surface lectins (1). The early works of Dr. A. Raz and colleagues [Meromsky et al. (4) and Raz and Lotan (9)] suggest an important role of soluble β-galactoside-specific lectins (galectins) in cancer cell adhesion and metastasis. Because the terminal residue of T antigen is β-galactose, one can reasonably suggest its possible interactions with members of the β-galactoside binding lectin family. Therefore, we studied the expression profiles of galectins, namely galectin-1, galectin-3, and galectin-4, in MDA-MB-435 cells. Our data indicated the abundant expression of ^{35}S-labeled galectin-1 and galectin-3 but not galectin-4 in these cells, which suggested a potential interplay of T antigen with galectins, most likely with galectin-3.

Both galectin-1 and galectin-3 appear to participate in the adhesion of the MDA-MB-435 cells to a monolayer of human endothelial cells as revealed by laser confocal microscopy. We observed the accumulation of the galectin-3 on endothelial cells at the sites of their contact with cancer cells, which would be supportive of possible interactions between T antigen and galectin-3. The T antigen-specific P-30 peptide was able to inhibit this adhesion by up to 50%.

The results presented in this paper demonstrate that β-galactoside-mediated, in particular T antigen-mediated, cell-cell interactions are important components of both the spontaneous homotypic aggregation of the MDA-MB-435 human breast carcinoma cells and their adhesion to the endothelium. The ability of P-30 to inhibit T antigen-mediated tumor cell aggregation and adhesion highlights its potential functional significance for antiadhesive therapy of cancer metastasis.

Materials and Methods

Cell Lines and Cultures. The MDA-MB-435 human breast carcinoma cell line, originally isolated from the pleural effusion of a patient with breast carcinoma, was kindly provided by Dr. Janet E. Price, M. D. Anderson Cancer Center, Houston, TX. This cell line was selected for our study because it was found to be highly metastatic in nude mice from mammary fat-pad tumors as well as on i.v. inoculation in vivo (14, 15) and exhibited superior aggregation and survivability in vitro compared with the other lines tested (16). Tumor cells were maintained in 5% CO_2/95% air at 37°C in a humidified incubator in tissue culture flasks as a monolayer culture using RPMI 1640 supplemented with L-glutamine, 10% fetal bovine serum, sodium pyruvate, and nonessential amino acids.

HUVECs pooled from multiple isolates were purchased from Cascade Biologicals, Inc. (Portland, OR). The cultures were free of HIV-1, Hepatitis B and C viruses, Mycoplasma, bacteria, yeast, and fungi. The cells were positive for the DiI-acetylated low density lipoprotein uptake and expression of von Willebrand factor and CD31 but not for the α-actin expression. The HUVECs were maintained on plastic as a monolayer culture in a humidified incubator in 5% CO_2/95% air at 37°C. The basal Medium 200 (Cascade Biologicals), supplemented with low serum growth supplement containing fetal bovine serum (2% v/v final concentration), hydrocortisone, human fibroblast growth factor, heparin, and human epidermal growth factor, was used. The cells at population doublings of approximately 8–12 were used for the adhesion experiments.

Peptide Synthesis and Purification. T antigen-binding peptide P-30 (HGRFILPWWYAFSPS) and control peptide (RRLLFYKYVYKRYRAG-KQRG) were chemically synthesized on the Applied Biosystems peptide synthesizer 431A using N-(9-fluorenyl)methoxycarbonyl-based chemistry and purified to homogeneity on a C-18 reverse-phase high-performance liquid chromatography column (ISCO Corp.).

Antibodies. A rabbit polyclonal anti-galectin-1 antiserum was a generous gift from Dr. Douglas W. N. Cooper (University of California, San Francisco,

CA). A rat monoclonal anti-galectin-3 (anti-Mac-2) antibody (17) was used as described previously (18). Rabbit anti-galectin-4 serum was raised using the COOH-terminal domain of rat intestinal galectin-4 as immunogen as described previously (19). Cy5-conjugated goat antirabbit IgG was purchased from Jackson Immuno Research Laboratories (West Grove, PA). Goat Texas Red-conjugated antirat antibody was purchased from Molecular Probes (Eugene, OR).

Cytochemical Analysis of T Antigen. The cytochemical analysis of T antigen was performed using PNA lectin-horseradish peroxidase conjugate, and subsequent color reaction was performed with diaminobenzidine tetrahydrochloride. The direct binding of T antigen-specific PNA lectin to MDA-MB-435 human breast carcinoma cells was performed as described previously (13) with one minor modification. After dissociation of cells from the plastic and before fixing them with 2% formaldehyde-PBS solution and placing on a microscope slide, the cells were allowed to aggregate for 30 min in serum-free RPMI 1640 at 37°C.

Cell Aggregation Assay. A homotypic aggregation assay of MDA-MB-435 cells was performed as previously described (4, 20). The only modification was made for the samples prepared for the cytological analysis of T antigen. In these experiments, cancer cells were allowed to aggregate for 30 min instead of 1 h to avoid formation of excessively large multicellular aggregates.

Analysis of Galectins Expression in MDA-MB-435 Cells. The metabolic [^{35}S]methionine/cysteine labeling of galectins followed by affinity purification on lactosyl-Sepharose and separation by SDS-PAGE was performed exactly as described previously (21). Densitometry of SDS-PAGE of the purified galectins was used to assess the relative amounts of each galectin. On the basis of the absolute yield of lactosyl-Sepharose purified galectins and the estimated volume of the confluent monolayer of MDA-MB-435 cells, the approximate molar concentrations of galectins 1, 3, and 4 were calculated as described previously (21).

Adhesion to the Endothelium. HUVECs were grown to confluence directly on microscope slides using the four-well Lab-Tec II chamber slide system (NalgeNunc, Naperville, IL). Twenty-four h before the adhesion experiment, the endothelial cell cultures were switched to quiescence medium (Medium 200 without low serum growth supplement), and MDA-MB-435 human breast carcinoma cells were prelabeled with 5 μg/ml solution of DiI (Molecular Probes) in serum-free RPMI 1640 for 60 min at 37°C. Immediately before the experiment, cancer cells were dissociated from plastic using a nonenzymatic cell dissociation reagent (Sigma, St. Louis, MO), and pipetted to produce a single-cell suspension. DiI-labeled breast carcinoma cells [5×10^4 cells per chamber in 2.5 ml of serum-free medium supplemented with various concentrations of P-30 (0 to 0.1 mg/ml) or control peptide] were added to the monolayer of the endothelial cells. The chambers were sealed with adhesive tape while ensuring that no air bubbles were trapped. The cells were allowed to adhere for 1 h at 37°C, after which the chambers were inverted and left upside down for 30 min to allow sedimentation of nonadhered cells. At the end of the incubation, the medium was drained while chambers were still upside-down. Samples were gently rinsed with PBS, fixed for 30 min in 2% formaldehyde solution in PBS, mounted under cover glass, and examined by fluorescent microscopy. Four random fields in each well were photographed at ×250, and the total number of adhered cells in every field was counted. The assay was performed in quadruplicate for each concentration of the peptides tested.

Laser Scanning Confocal Microscopy. The samples for laser scanning confocal microscopy were prepared exactly as described above in "Adhesion to the Endothelium," except that the cancer cells used in these experiments were not prelabeled with DiI, and samples were fixed (but not permeabilized) in 2% formaldehyde solution in PBS for 24 h. The antibodies against galectins-1, -3, and -4 were used as described previously (20). The goat Texas-Red-conjugated antirat antibody and Cy5-conjugated goat antirabbit IgG were used as secondary antibodies at a dilution of 1:100. The laser scanning confocal microscopy was performed with a Bio-Rad MRC 600 confocal system. The RHS and YHS blocks were used to detect fluorescence emitted by Cy5 and Texas Red respectively. The Z stacks were prepared by obtaining serial sections with 0.5-μm increments and analyzed in orthogonal projections (Y-Z and X-Z sections) using the MetaMorph Imaging System software (Universal Imaging, Hallis, NH).

Results and Discussion

Involvement of T Antigen in Homotypic Aggregation of MDA-MB-435 Human Breast Carcinoma Cells. Multicellular aggregate formation is an important feature of metastatic cancer cells directly correlating with their increased survival potential *in vitro* (20) and metastatic propensity *in vivo* (22). The cancer-associated T antigen has been implicated in tumor cell adhesion through carbohydrate-lectin interactions (6, 23). We previously reported the expression of large quantities of T antigen on the surface of MDA-MB-435 cells that was confirmed by the binding of T antigen-specific PNA lectin (13). In this study, we investigated the role of T antigen in homotypic aggregation of the MDA-MB-435 breast cancer cells. Tumor cells collected from subconfluent (70–80%) cultures were allowed to form multicellular aggregates as described in "Materials and Methods." The direct binding of T antigen-specific PNA lectin, conjugated to horseradish peroxidase followed by color reaction with diaminobenzidine tetrahydrochloride, was used to visualize T antigen. The cytochemical analysis of the samples that contained multicellular aggregates revealed significant accumulation of T antigen at the sites of cell contacts (Fig. 1A), which suggested participation of T antigen in homotypic aggregation of MDA-MB-435 breast carcinoma cells. Consistent with this is the fact that the addition of different concentrations of synthetic T antigen-specific peptide, P-30 (HGRFILPW-WYAFSPS), inhibited homotypic aggregation of MDA-MB-435 cells in a dose-dependent manner (Fig. 1B). A maximal inhibitory effect (>70%) was achieved at a peptide concentration of 0.1 mg/ml. The control peptide (RRLLFYKYVYKRYRAGKQRG), which does not interact with T antigen (13), failed to inhibit homotypic aggregation of MDA-MB-435 cells (Fig. 1, C–E). These findings, as well as the previously reported ability of P-30 to inhibit asialofetuin-mediated
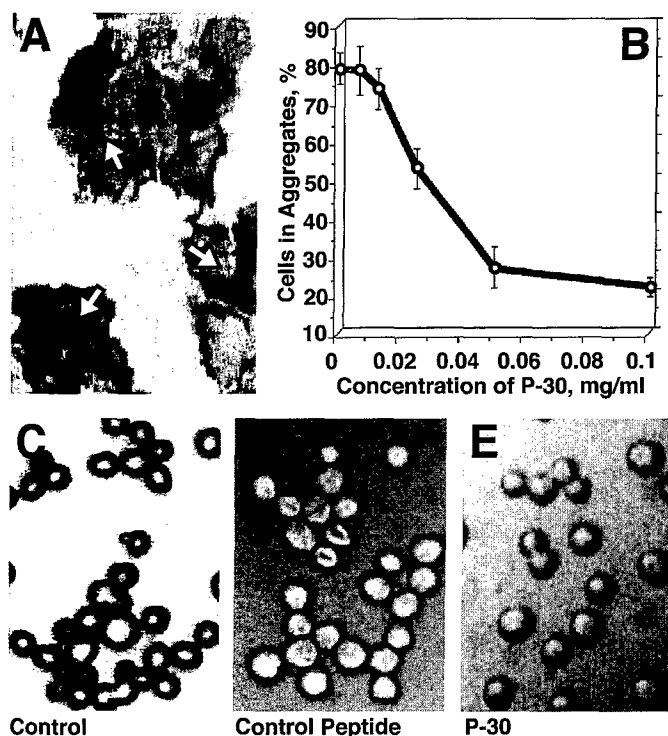

Fig. 2. [^{35}S]Methionine/cysteine-labeled expression profile of β-galactoside-specific lectins (galectins) in MDA-MB-435 human breast carcinoma cells. *On the left*, the position of the molecular weight markers (*46*, *29*, and *14*, for M_r 46,000, 29,000, and 14,000, respectively).There is an abundant expression of galectin-1 and galectin-3 compared with a very weak expression of galectin-4. The additional weak band corresponding to the molecular weight of approximately M_r 40,000 suggests a low level of expression of an unidentified soluble β-galactoside-specific lectin (*Gal-X*).

aggregation of mouse melanoma cells (13), suggest that the effect of P-30 on homotypic aggregation of MDA-MB-435 cells is T antigen-specific.

Expression of β-Galactoside-specific Lectins (Galectins) on MDA-MB-435 Cells. Because T antigen (Galβ1 → 3GalNAc) has β-galactose as a terminal sugar, it is likely that T antigen-mediated interactions may involve the participation of β-galactoside-specific lectins (galectins). Thus, we studied the expression profile of the galectins, namely galectin-1, galectin-3, and galectin-4 in MDA-MB-435 cells. Metabolic [^{35}S]methionine/cysteine labeling followed by affinity purification on lactosyl-Sepharose and separation by SDS-PAGE was used to isolate galectins and characterize their expression in this cell line. The results of these experiments (Fig. 2) identified galectin-1 as a major β-galactoside-specific lectin expressed in MDA-MB-435 breast carcinoma cells. The estimated molar concentrations of galectins-1, -3, and -4 in MDA-MB-435 cells were in the range of 1–3 μM, 100–500 nM, and 10–50 nM, respectively. The presence of the additional minor band corresponding to a molecular weight of M_r ~40,000 (Fig. 2) suggests the weak expression of another, yet unidentified, soluble lactose-binding lectin (Gal-X). Human galectin-3 displays a 20-fold higher specific activity in binding to the Galβ1→3GalNAc disaccharide than galectin-1 (24). Thus, galectin-3 is most likely to interact with T antigen. Previously reported inhibition by T antigen-specific P-30 of asialofetuin-mediated aggregation of B16-F1 cells (13), known to be galectin-3-dependent (25), is also supportive of this interaction. The analysis of β-galactoside-binding lectins in 11 other human breast carcinoma cell lines established from pleural or ascitic effusions revealed similar galectin expression profiles,[4] which suggests that galectin-1 and galectin-3 overexpression is a phenomenon frequently occurring in metastatic breast cancer.

Adhesion of MDA-MB-435 Breast Carcinoma Cells to the Endothelium. Both galectin-1 and galectin-3 were found to be expressed on the endothelium of various origins in different species including humans (26). Galectin-1 was also shown to participate in murine RAW117-H10 large-cell lymphoma cell adhesion to liver microvessel endothelial cells (26), and galectin-3 was suggested to be, at least in part, responsible for the preferential adhesion of prostate cancer

Fig. 1. *A*, direct binding of T antigen-specific PNA to the MDA-MB-435 human breast carcinoma cells. *Arrows*, accumulation of T antigen at the sites of the cell-cell contact. *B*, dose-dependent inhibition of spontaneous homotypic aggregation of the MDA-MB-435 human breast carcinoma cells by T antigen-specific peptide P-30. *C–E*, inhibition of spontaneous homotypic aggregation of MDA-MB-435 human breast carcinoma cells by 0.1 mg/ml of synthetic P-30 (*E*) but not by the same concentration of the control peptide (*D*) compared with the control (*C*).
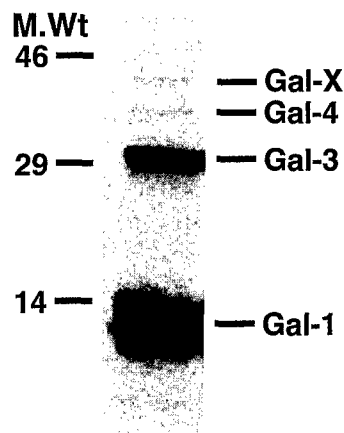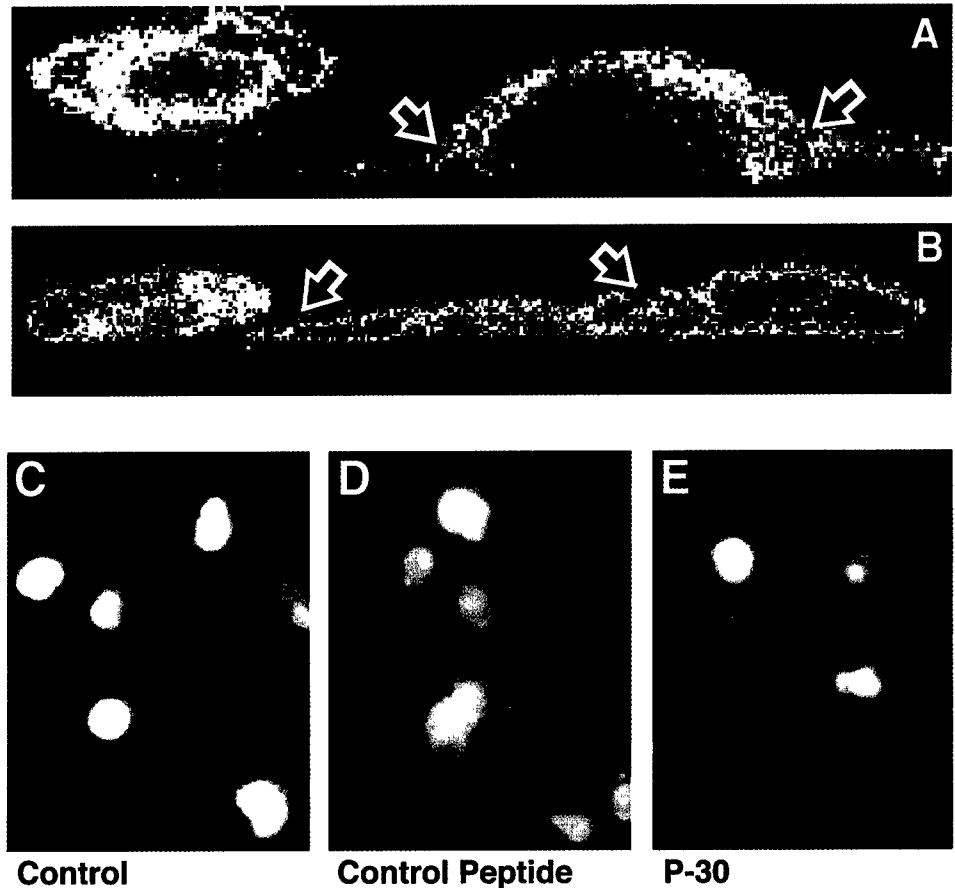
Fig. 3. Involvement of the galectin-1 (*A*) and galectin-3 (*B*) in the adhesion of the MDA-MB-435 human breast carcinoma cells to the monolayer of human umbilical endothelial cells as revealed by laser confocal microscopy. The X-Z sections shown were obtained as described in "Materials and Methods" using a ×60 lens. The images were pseudocolored (*green*, galectin-1; *red*, galectin-3). *Arrows*, clustering toward the cell contacts of galectin-1 on cancer cells (*A*) and of galectin-3 on endothelial cells (*B*). The superimposed fluorescent photomicrographs of DiI-labeled MDA-MB-435 breast cancer cells adhered to the monolayer of HUVEC cells (*C–E*). There is an inhibition of the adhesion by 0.1 mg/ml of the T antigen-specific synthetic P-30 (*E*) but not by the same concentration of the control peptide (*D*) compared with the control (*C*).

cells to human bone marrow endothelial cells (27). Thus, it was of interest to analyze whether β-galactoside-specific lectins participate in adhesion of the MDA-MB-435 cells to the endothelium. Confocal laser microscopy revealed the clustering of both galectin-1 and galectin-3 to the sites of contact between MDA-MB-435 cells and human umbilical endothelial cells (Fig. 3, *A* and *B*) indicative of their involvement in the interaction between cancer and endothelial cells. We could not observe, however, any sign of galectin-4 participation in this process, which was consistent with the data on its low level of expression in MDA-MB-435 cells.

Interestingly, galectin-1 and galectin-3 reacted differently on tumor and endothelial cells. A strong galectin-1 signal accumulated at the sites of tumor-endothelial cell contact predominantly on the cancer cells (Fig. 3*A*), which suggested the involvement of one or more of its cognate ligands on the endothelium. Galectin-3, in contrast, although also being strongly expressed on the tumor cells, clearly demonstrated signal accumulation toward the sites of the cell contact on HUVEC (Fig. 3*B*) possibly interacting with T antigen or other putative ligands on cancer cells. We hypothesized that if galectin-3 on the endothelial cells interacts with T antigen on MDA-MB-435 cells, then T antigen-specific P-30 should inhibit this interaction as it did in the case of homotypic aggregation. Thus, we performed experiments in which cancer cells were allowed to adhere to a monolayer of endothelial cells in the presence of P-30 (0.1 mg/ml final concentration) or a control peptide of identical concentration. The results of these experiments (Fig. 3, *C–E*) showed that the control peptide did not effect the adhesion of the MDA-MB-435 cells to the endothelial cells (Fig. 3, *C* and *D*), whereas T antigen-specific P-30 significantly (2-fold) inhibited it (Fig. 3*E*). When adhesion experiments were performed with different concentrations of P-30, we found the peptide's effect to be dose-dependent with the maximal inhibition achieved up to 50% (Fig. 4). These data demonstrated that adhesion of the MDA-MB-435

human breast carcinoma cells to the endothelial cells was, at least in part, mediated by T antigen. We observed the same inhibitory effects of the P-30 peptide on both adhesion to the endothelium and spontaneous homotypic aggregation of DU-145 human prostate carcinoma cells (data not shown), which suggests that similar molecular mech-

P-30 concentration, mg/ml
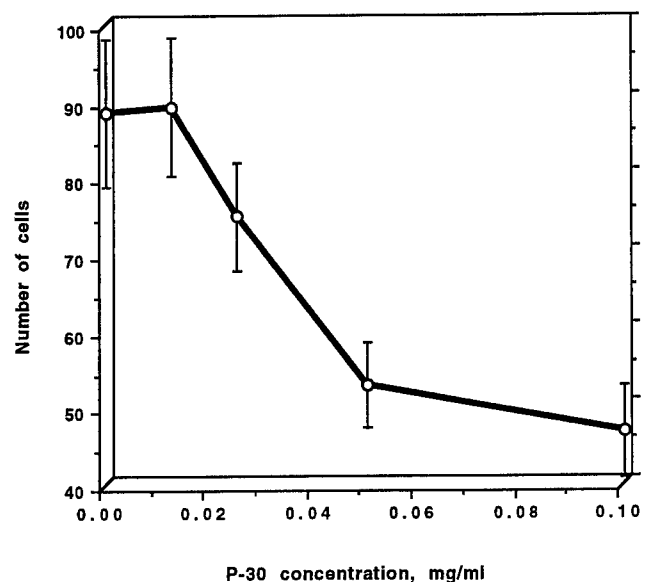
Fig. 4. Dose-dependent inhibition of the adhesion of MDA-MB-435 human breast carcinoma cells to the endothelium by synthetic T antigen-specific peptide P-30. The maximum inhibitory effect (about 50%) was achieved at 0.1 mg/ml concentration of the peptide. Representative results from one of three similar experiments are presented as mean of quadruplicate determinations. *Bars*, SD.

anisms of adhesion could be involved in different human malignancies.

Multicellular aggregate formation and adhesion of tumor cells to the endothelium are crucial events during early stages of cancer metastasis. Taken together, our data indicate that β-galactoside and particularly T antigen-mediated cell-cell interactions are important components of these events. To the best of our knowledge, this is the first observation that directly shows the accumulation of galectin-1 and galectin-3 at sites of contact between cancer and endothelial cells, which is indicative of their active participation in the adhesion of tumor cells to the endothelium.

Strikingly different behavior of these two β-galactoside-specific lectins reflects the complexity of the adhesion process. The accumulation of galectin-1 at the sites of cell-cell contacts predominantly on cancer cells and galectin-3 on endothelial cells suggests that several of their cognate ligands may be simultaneously involved here on both tumor and endothelial cells. Inhibition of tumor cell adhesion by the T antigen-specific P-30 peptide, however, highlights an active role for this cell surface carbohydrate structure in cancer-endothelial cell interactions. Recent observations of Al-Mehdi et al. (7) indicate that hematogenous metastases arise from the endothelium-attached tumor cells, which makes them particularly vulnerable to intravascular drugs capable of disrupting cancer-endothelial cell interactions. The ability of a short synthetic peptide to effectively interfere with this line of intercellular communication may also be of functional significance for the development of new antiadhesive therapies of cancer metastasis.

Two other types of compounds that also target β-galactoside-mediated adhesion have already been proven to be effective inhibitors of cancer metastases in vivo (28, 29). Specifically, synthetic analogues of naturally occurring conjugates of carbohydrates and amino acids (glycoamines) were shown to inhibit up to 75% both the incidence and number of MDA-MB-435 human breast cancer metastases in nude mice experiments (28). Modified citrus pectin, as reported by Pienta et al. (29), was also demonstrated to be an effective inhibitor of B16-F1 murine melanoma lung colonization as well as MAT-LyLu Dunning rat prostate cancer metastasis. Both synthetic glycoamines and modified citrus pectin act through the interaction with β-galactoside-specific lectins, specifically galectin-3, presumably by mimicking corresponding glycoepitopes of the cell surface glycomacromolecules or circulating glycoproteins (30). It is reasonable to hypothesize that the development of molecules directed against appropriate carbohydrate structures may likewise lead to the development of new effective antiadhesive therapies of cancer metastases.

This suggests new approaches to the concept of antiadhesive therapy of cancer (reviewed in Ref. 31), originally developed by early pioneering works of Dr. R. Kerbel and colleagues (32–34) and Dr. A. Raz and colleagues [Meromsky et al. (4 and Inohara and Raz (25)]. Traditional approaches to such therapy would be to generate appropriate sugar-specific antibodies. The difficulties of raising highly specific antibodies against carbohydrate moieties, as well as of the large-scale production of such antibodies, are well known, however. The development of carbohydrate-specific synthetic peptides using combinatorial bacteriophage display libraries could be a valid complimentary approach.

Acknowledgments

References

1. Hakomori, S-I. Aberrant glycosylation in tumors and tumor-associated carbohydrate antigens. Adv. Cancer Res., 52: 257–331, 1989.
2. Hakomori, S-I. Possible functions of tumor-associated carbohydrate antigens. Curr. Opin. Immunol., 3: 646–653, 1991.
3. Glaves, D. Correlation between circulating cancer cells and incidence of metastasis. Br. J. Cancer, 48: 665–673, 1983.
4. Meromsky, L., Lotan, R., and Raz, A. Implications of endogenous tumor cell surface lectins as mediators of cellular interactions and lung colonization. Cancer Research, 46: 5270–5275, 1986.
5. Springer, G. F., and Desai, P. R. Common precursors of human blood group MN specificities. Biochem. Biophys. Res. Commun., 61: 470–475, 1974.
6. Springer, G. F., Cheingsong-Popov, R., Schirrmacher, V., Desai, P. R., Tegtmeyer, H. Proposed molecular basis of murine tumor cell-hepatocyte interaction. J. Biol. Chem., 258: 5702–5706, 1983.
7. Al-Mehdi, A. B., Tozawa, K., Fisher, A. B., Shientag, L., Lee, A., and Muschel, R. J. Intravascular origin of metastasis from the proliferation of endothelium-attached tumor cells: a new model for metastasis. Nat. Med., 6: 100–102, 2000.
8. Springer, G. F. T and Tn, general carcinoma autoantigens. Science (Washington DC) 224: 1198–1206, 1984.
9. Raz, A., and Lotan, R. Endogenous galactoside-binding lectins: a new class of functional tumor cell surface molecules related to metastasis. Cancer Metastasis Rev., 6: 433–452, 1987.
10. Springer, G. F., Desai, P. R., Ghazizadeh, M., and Tegtmeyer, H. T/Tn pancarcinoma autoantigens: fundamental, diagnostic, and prognostic aspects. Cancer Detect. Prev., 19: 173–182, 1995.
11. Springer, G. F. Tn epitope (N-acetyl-D-galactosamine α-O-serine/threonine) density in primary breast carcinoma: a functional predictor of aggressiveness. Mol. Immunol., 26: 1–5, 1989.
12. Peletskaya, E. N., Glinsky, G. V., Deutscher, S. L., and Quinn, T. P. Identification of peptide sequences that bind the Thomsen-Friedenreich cancer-associated glycoantigen from bacteriophage peptide display libraries. Mol. Diversity, 2: 13–18, 1996.
13. Peletskaya, E. N., Glinsky, V. V., Glinsky, G. V., Deutscher, S. L., and Quinn, T. P. Characterization of peptides that bind the tumor-associated Thomsen-Friedenreich antigen selected from bacteriophage display libraries. J. Mol. Biol. 270: 374–384, 1997.
14. Zhang, R. D., Fidler, I. J., and Price, J. E. Relative malignant potential of human breast carcinoma cell lines established from pleural effusion and a brain metastasis. Invasion Metastasis, 11: 204–215, 1991.
15. Price, J. E., Polyzos, A., Zhang, R. D., and Daniels, L. M. Tumorigenicity and metastasis of human breast carcinoma cell lines in nude mice. Cancer Res., 50: 717–721, 1990.
16. Glinsky, G. V., Glinsky, V. V., Ivanova, A. B., and Hueser, C. J. Apoptosis and metastasis: increased apoptosis resistance of metastatic cancer cells is associated with the profound deficiency of apoptosis execution mechanisms. Cancer Lett., 115: 185–193, 1997.
17. Ho, M.-K., and Springer, T. A. Mac-2, a novel 32,000 M_r mouse macrophage subpopulation-specific antigen defined by monoclonal antibodies. J. Immunol., 128: 1221–1228, 1982.
18. Huflejt, M. E., Turck, C. W., Lindstedt, R., Barondes, S. H., and Lefler, H. L-29, a soluble lactose-binding lectin, is phosphorylated on serine 6 and serine 12 in vivo and by casein kinase I. J. Biol. Chem., 268: 26712–26718, 1993.
19. Oda, Y., Hermann, J., Gitt, M. A., Turck, C. W., Burlingame, A. L., Barondes, S. H., and Lefler, H. Soluble lactose-binding lectin from rat intestine with two different carbohydrate-binding domains in the same peptide chain. J. Biol. Chem., 268: 5929–5939, 1993.
20. Glinsky, G. V., and Glinsky, V. V. Apoptosis and metastasis: a superior resistance of metastatic cancer cells to programmed cell death. Cancer Lett., 101: 43–51, 1996.
21. Huflejt, M. E., Jordan, E. T., Gitt, M. A., Barondes, S. H., and Lefler, H. Strikingly different localization of galectin-3 and galectin-4 in human colon adenocarcinoma T84 cells. J. Biol. Chem., 272: 14294–14303, 1997.
22. Fidler, I. J. The relationship of embolic homogeneity, number, size and viability to the incidence of experimental metastasis. Eur. J. Cancer, 9: 223–227, 1975.
23. Kishikawa, T., Ghazizadeh, M., Sasaki, Y., and Springer, G. F. Specific role of T and Tn tumor-associated antigens in adhesion between a human breast carcinoma cell line and a normal human breast epithelial cell line. Jpn. J. Cancer Res., 90: 326–332, 1999.
24. Sparrow, C. P., Leffler, H., and Barondes, S. H. Multiple soluble β-galactoside-binding lectins from human lung. J. Biol. Chem., 262: 7383–7390, 1987.
25. Inohara, H., and Raz, A. Effects of natural complex carbohydrate (citrus pectin) on murine melanoma cell properties related to galectin-3 functions. Glycoconj. J., 11: 527–532, 1994.
26. Lotan, R., Belloni, P. N., Tressler, R. J., Lotan, D., Xu, X. C., and Nicolson, G. L. Expression of galectins on microvessel endothelial cells and their involvement in tumor cell adhesion. Glycoconj. J., 11: 462–468, 1994.
27. Lehr, J. E., and Pienta, K. J. Preferential adhesion of prostate cancer cells to a human bone marrow endothelial cell line. J. Natl. Cancer Inst., 90: 118–123, 1998.
28. Glinsky, G. V., Price, J. E., Glinsky, V. V., Mossine, V. V., Kiriakova, G., and Metcalf, J. B. Inhibition of human breast cancer metastasis in nude mice by synthetic glycoamines. Cancer Res., 56: 5319–5324, 1996.
29. Pienta, K. J., Naik, H., Akhtar, A., Yamazaki, K., Replogle, T. S., Lehr, J., Donat, T. L., Tait, L., Hogan, V., and Raz, A. Inhibition of spontaneous metastasis in rat prostate cancer model by oral administration of modified citrus pectin. J. Natl. Cancer Inst., 87: 348–353, 1995.
30. Inohara, H., Akahani, S., Koths, K., and Raz, A. Interactions between galectin-3 and Mac-2-binding protein mediate cell-cell adhesion. Cancer Res., 56: 4530–4534, 1996.
31. Glinsky, G. V. Anti-adhesion cancer therapy. Cancer Metastasis Rev., 17: 177–185, 1998.
32. Kerbel, R. S., Rak, J., Kobayashi, H., Man, M. S., St. Croix, B., and Graham, C. H. Multicellular resistance: a new paradigm to explain aspects of acquired drug resistance of solid tumors. Cold Spring Harbor Symp. Quant. Biol., 59: 661–672, 1994.
33. Kerbel, R. S., St. Croix, B., Rak, J., and Graham, C. H. Is there a role for anti-adhesives as chemosensitizers in the treatment of solid tumors by chemotherapy? Bull. Inst. Pasteur, 92: 248–256, 1995.
34. Kerbel, R. S., St. Croix, B., Florenes, V. A., and Rak, J. Induction and reversal of cell adhesion-dependent multicellular drug resistance in solid breast tumors. Hum. Cell, 9: 257–264, 1996.

The Role of Thomsen-Friedenreich Antigen in Adhesion of Human Breast and Prostate Cancer Cells to the Endothelium

Vladislav V. Glinsky[1,2], Gennadi V. Glinsky[3,4], Kate Rittenhouse-Olsen[5], Margaret E. Huflejt[3], Olga V. Glinskii[1], Susan L. Deutscher[1], and Thomas P. Quinn[1]

[1]*Department of Biochemistry, University of Missouri, Columbia, MO 65211*

[2]*Cancer Research Center, Columbia, MO 65201*

[3]*Sidney Kimmel Cancer Center and* [4]*Metastat, Inc., San Diego, CA 92121*

[5]*Department of Biotechnical and Clinical Laboratory Science, State University of New York at Buffalo, Buffalo, NY 14214*

Correspondence should be addressed to T.P.Q.; email: QuinnT@missouri.edu or V.V.G.; email: glinskiivl@missouri.edu

Abstract

Interactions of metastatic cancer cells with vasculatory endothelium are critical during early stages of cancer metastasis. Understanding the molecular underpinnings of these interactions is essential for the development of new efficacious cancer therapies. Here we demonstrate that cancer-associated carbohydrate T antigen plays a leading role in docking breast and prostate cancer cells onto endothelium by specifically interacting with endothelium-expressed β-galctoside-binding protein, galectin-3. Importantly, T antigen-

1

bearing glycoproteins are also capable of mobilizing galectin-3 to the surface of endothelial cells thus priming them for harboring metastatic cancer cells. The T antigen-mediated tumor-endothelial cell interactions could be efficiently disrupted using synthetic compounds either mimicking or masking this carbohydrate structure. High efficiency of T antigen-mimicking and T antigen-masking inhibitors of tumor cell adhesion warrants their further development into anti-adhesive cancer therapeutics.

Introduction

Metastasis is a major fatal complication associated with human malignant disorders. Recent findings demonstrate that hematogenous cancer metastases originate from intravascular growth of endothelium-attached rather than extravasated cancer cells[1], highlighting the key role of tumor-endothelial cell interactions in cancer metastasis. Understanding the molecular mechanisms of these interactions is crucial for the development of new efficacious cancer therapies. A broad array of adhesion molecules such as carbohydrates, lectins, cadherins, and integrins have been implicated in the adhesion of tumor cells to the vasculatory endothelium. This reflects a complexity of the adhesion process. Moreover, different adhesion molecules have been shown to participate at distinct stages in a multistep binding process[2]. For example, selectins were shown to contribute to the initial contact of circulating cells with endothelium by inducing their rolling[3], while galectin-3 has been proposed to participate in docking of cancer cells on capillary endothelium[4], and integrins were demonstrated to play a role in the development of more stable attachment involving protein-protein interactions[3].

Among all the variety of adhesion molecules, cell surface carbohydrate structures have been a focus of many investigative efforts into their roles in cancer cell adhesion and metastasis. Aberrations in cell surface carbohydrates, emblematic of malignant transformation, have been shown to facilitate tumor cell colonization and metastasis by effecting normal cell-cell interactions[5,6]. One of the most widely distributed cancer-associated cell surface carbohydrate moieties is the pancarcinoma T antigen[7]. T antigen is a simple mucin-type disaccharide[8], Galβ1-3GalNAc, expressed on the outer cell surfaces of T-cell lymphomas and most human carcinomas[7-9] including breast and prostate[10]. The role for T antigen in tumor cell adhesion and metastasis has been proposed based on the existence of T antigen-mediated adhesion of highly metastatic murine lymphoma cells and hepatocytes[9]. Recently we demonstrated the participation of T antigen in human breast carcinoma cell adhesion to the endothelium[11]. We also reported that a 15-amino acid T antigen-specific peptide, P-30 (HGRFILPWWYAFSPS), selected from a bacteriophage display library[22,23], specifically and significantly (>50%) inhibited adhesion of human breast cancer cells to the endothelium[11]. These results underscored the importance of T antigen-mediated interactions in breast cancer metastasis. However, the molecular mechanisms of T antigen-mediated adhesion as well as cognate physiological receptors for T antigen have not been identified.

Based on the fact that the terminal residue of T antigen is β-galactose, we suggested its potential interactions with galectin-3[11], a $M_r \sim 30,000$ member of a family of soluble β-galactoside-specific lectins[12,13]. Although the physiological role of this carbohydrate-binding protein is still greatly debated, galectin-3 has been implicated in several distinct fundamental cellular processes such as pre-mRNA splicing[14], cell growth and

differentiation[15], regulation of apoptosis[16,17], and cell-cell recognition and adhesion[17,18].

In several experimental systems, the expression of galectin-3 in cancer cells was

associated with increased malignant and metastatic phenotype[20,21]. Moreover,

preferential adhesion of PC-3 human prostate cancer cells to bone marrow endothelial

cells was found to be at least in part galectin-3-dependent[4]. Recently, we demonstrated

the involvement of the endothelium-expressed galectin-3 in breast carcinoma-endothelial

cell adhesion[11] supportive of a possible interaction of this β-galactoside-binding lectin

with T antigen.

We hypothesized that if T antigen is indeed interacting with galectin-3 during tumor

cell docking onto the endothelium, it could be a common molecular mechanism of cancer

cell adhesion pertinent to a metastatic dissemination of a variety of T antigen-expressing

human malignancies. Carbohydrate-lectin interactions are believed to take place during

an initial reversible phase of cell adhesion that determines cell-cell recognition

specificity[26,27]. The efficient specific blockage of these early binding events may

significantly modify the outcome of the adhesion and affect the metastatic process in

whole.

In this study, we demonstrate that two synthetic inhibitors of T antigen-mediated

adhesion, the T antigen-binding P-30 peptide, and a sugar based T antigen mimetic,

lactulosyl-L-leucine, efficiently (43-56%) inhibit the adhesion of breast and prostate

cancer cells to human endothelium. Both T antigen-masking P-30 and T antigen-

mimicking lactulosyl-L-leucine display the same maximal inhibitory effect on adhesion

of breast and prostate cancer cells as a highly specific anti-T antigen monoclonal

antibody does. The results of inhibition ELISA experiments confirm the specificity of

both synthetic inhibitors, and demonstrate direct binding of the recombinant human galectin-3 to the protein-linked T-antigen. Remarkably, endothelial cells exhibit rapid and marked increase in cell surface galectin-3 expression when treated with T antigen-bearing glycoproteins. This result suggests a novel function for circulating T antigen-expressing glycoproteins such as cancer-associated mucin, which may act by priming capillary endothelium for harboring cancer cells.

The results presented in this paper define T antigen as one of the leading factors during early stages of breast and prostate cancer-endothelial cell interactions. We demonstrate that T antigen is acting both as a major cell surface carbohydrate ligand for galectin-3 on breast and prostate cancer cells, and as a factor causing mobilization of galectin-3 to the outer membrane on endothelial cells. The significance of T antigen-mediated adhesion in breast and prostate cancer identifies T antigen-galectin-3 interactions as a valid target for development of new anti-adhesive therapies of cancer metastases.

Results and Discussion

T Antigen Expression. The expression of T antigen in breast cancer tissues is well documented and is associated with tumor progression and metastasis[24]. However, this carbohydrate structure is not only specific to breast cancer. Rather, it is characteristic of a vast majority of human adenocarcinomas. Similarly, T antigen is often detectable in prostate cancer lesions (Fig. 1, A). Furthermore, in patients with prostate carcinoma, the expression of T antigen has also been found to correlate with tumor grade and metastasis[10,25]. Both breast (MDA-MB-435) and prostate (DU-145) cancer cell lines used in this study express T antigen on their surfaces. We previously demonstrated the

presence of T antigen on MDA-MB-435 human breast carcinoma cells[23]. This cell line, originally isolated from the pleural effusion of a patient with breast cancer, has been shown to be highly metastatic in nude mice[28.29]. The fact that adhesion of MDA-MB-435 cells to the endothelium could be efficiently (two-fold) inhibited by the T antigen-binding P-30 peptide[11] is indicative of the importance of T antigen in breast cancer-endothelial cell interactions. The DU-145 human prostate carcinoma cell line, chosen for our experiments, was also originally isolated from a metastatic lesion[30]. Importantly, this cell line retains its metastatic potential, as reflected in the ability of DU-145 cells to develop metastasis in nude mice[31]. In this study we show that similar to MDA-MB-435 metastatic breast cancer cells, the DU-145 human prostate carcinoma cells also express T antigen on their surfaces (Fig. 1, B). This observation suggests that T antigen might likewise participate in prostate cancer cell adhesion to the endothelium. To address this question we investigated whether compounds, capable of specifically masking T antigen, would interfere with prostate cancer-endothelial cell interactions.

Inhibition of Cancer Cell Adhesion to the Endothelium by Masking T Antigen. The T antigen-specific P-30 peptide (HGRFILPWWYAFSPS), was originally isolated from a bacteriophage display library[22]. The synthetic P-30 binds with high affinity and specificity to both free T antigen disaccharide in solution and T antigen-bearing glycoproteins[23]. It is also capable of specifically recognizing T antigen-expressing cancer cells of different origin[22,23], and efficiently inhibiting asialofetuin-mediated cancer cell aggregation[23] and breast carcinoma cell adhesion to the endothelium[11]. Our previous results suggest that the peptide is masking T antigen epitopes on cancer cells thus

6

preventing interactions with their cognate ligands. In this study, we used the T antigen-masking P-30 peptide to investigate if T antigen participates in prostate cancer cell adhesion to the endothelium. We studied the effect of different concentrations (0 to 0.1 mg/ml) of synthetic T antigen-specific P-30 on adhesion of DU-145 human prostate carcinoma cells to a monolayer of human umbilical vein endothelial cells (HUVEC). The results of these experiments (Fig. 2, A-H) showed that P-30 inhibited the adhesion of both DiI (1,1'-dioctadecyl-3, 3, 3', 3'-tetramethylindocarbocyanine)- (Fig. 2, A) and acridine orange- (Fig. 2, B-G) labeled DU-145 cells to endothelial cells in a dose-dependent manner, whereas the control peptide (RRLLFYKYVYKRYRAGKQRG) failed to inhibit adhesion (Fig. 2, H). To assess the efficiency of T antigen masking by P-30 peptide, we compared the maximal inhibitory effects on breast and prostate cancer cell binding to the endothelium, achievable with P-30 and an anti-T antigen antibody. A monoclonal antibody to irrelevant plant protein was used as a control in these experiments. We found that the control antibody did not inhibit attachment of tumor cells to HUVEC (Fig. 2, I and J), while both anti-T antigen antibody and P-30 exhibited almost identical maximal inhibitory effect on breast (Fig. 2, I) and prostate (Fig. 2, J) cancer cell adhesion. The results of these experiments demonstrated that synthetic P-30 peptide was masking T antigen as efficiently as the highly specific monoclonal anti-T antigen antibody. However, neither P-30 nor anti-T antigen antibody inhibited tumor cell adhesion to the endothelium completely. The inhibition efficiency (ranging from 43% to 56% in different experiments) displayed by these two compounds, most likely reflected the impact of T antigen-mediated interactions in our experimental system. Apparently, different adhesion molecules such as integrins might also contribute to the binding. It has

been suggested that circulating metastatic cells interact with endothelium in two distinct stages[26], the initial reversible docking stage, mediated by carbohydrate-lectin interactions, and the second stabilizing integrin-mediated locking stage, which requires more prolonged cell contact[27]. In our adhesion experiments, cancer and endothelial cells were in physical contact for 1 h, allowing sufficient time for integrin-mediated binding events to occur. Supportive of this suggestion are results reported by Lehr and Pienta[4] employing a similar experimental design. They demonstrated that antibodies to different members of the integrin family such as CD11a, CD18, and LFA-1, inhibited adhesion of PC-3 prostate cancer cells to endothelium from 20% to 55%, suggesting the importance of integrins in stabilizing adhesion of tumor cells docked onto the endothelium. In contrast, interactions between T antigen and the corresponding carbohydrate-binding lectin(s) preceding integrin-mediated adhesion, most likely are crucial during an initial docking stage. Supportive of this idea are the results of experiments employing *in flow* experimental systems[32], showing that under conditions of flow, anti-integrin antibodies do not affect the adhesion of MDA-MB-435 breast carcinoma cells to the endothelium, whereas the synthetic T antigen mimetic lactulosyl-L-lecine inhibits it up to 80%. These results imply that T antigen- but not integrin-mediated interactions play significant role in initiating cancer cell binding to the endothelium.

Inhibition of Cancer Cell Adhesion to the Endothelium by Mimicking T Antigen.
An independent approach to the study of T antigen-mediated adhesion would be to use compounds capable of mimicking T antigen. One such compound is a synthetic carbohydrate-amino acid conjugate (glycoamine), *N*-(1-Deoxy-4-*O*-(β-D-galactopyranos-

1-yl)-D-fructofuranos-1-yl)-(S)-2-amino-4-methylpentanoic acid (lactulosyl-L-leucine).

Lactulosyl-L-leucine is capable of targeting β-galactoside-binding lectins (galectins) by

mimicking the corresponding carbohydrate epitopes of naturally occurring

glycoproteins[33]. Similarly to P-30, lactulosyl-L-leucine efficiently inhibits asialofetuin-

mediated cancer cell aggregation and competes with T antigen-specific PNA lectin for

binding to breast carcinoma cells[34]. In this study, we report that lactulosyl-L-leucine

likewise inhibited the adhesion of breast (Fig. 3, E, F) and prostate (data not shown)

tumor cells to the endothelium. The inhibition efficiency of this compound, 52% and

54% for breast and prostate carcinoma cells respectively, was similar to that of the P-30

peptide and the anti-T antigen antibody. However, unlike P-30, lactulosyl-L-leucine is

acting not through masking, but through mimicking T antigen. The T antigen mimetic

properties of lactulosyl-L-leucine are evident in its ability to compete off binding of T

antigen to cancer cells (Fig. 3, A-C) and T antigen-specific PNA lectin to asialofetuin

(Fig. 3, D, iv, v). Interestingly, the substitution of lactulosyl for lactitol completely

abolishes the ability of the resulting compound, lactitol-L-leucine, to both mimic T

antigen (Fig.3, D, vi) and inhibit tumor cell adhesion to the endothelium (Fig. 3, G).

These results demonstrate that the anti-adhesive properties of lactulosyl-L-leucine strictly

depend on the compound's carbohydrate moiety and aptitude to mimic T antigen.

Importantly, this T antigen-mimicking compound was already shown to inhibit up to 75%

both the incidence and number of breast cancer metastases in nude mice experiments[34].

This finding highlights the critical role of T antigen-mediated interactions in the

metastatic process. The molecular basis of these interactions is still poorly understood,

however. The identification of the molecules acting as T antigen receptors in cancer-endothelial cell adhesion will be of utmost interest.

Interaction of T Antigen with Galectin-3. Since the terminal sugar of T antigen is β-galactose, the involvement of β-galactoside-binding lectins (galectins) in T antigen-mediated adhesion was investigated. Two out of nine currently known galectins, namely galectin-1 and -3, were previously found to be most prominently expressed in cancer and endothelial cells, and were implicated in cancer cell adhesion[35-37]. Based on the fact that human galectin-3 exhibits 200-fold higher specific activity toward Galβ1-3GalNAc disaccharide than galectin-1[12], we previously proposed the interaction of T antigen with galectin-3 during cancer cell adhesion to the endothelium[11]. Supportive of this interaction is the observation reported by Bresalier et al.[38] that colon cancer mucin, a glycoprotein most often decorated with multiple T antigen epitopes, serves as a specific ligand for galectin-3. Moreover, they also demonstrated that fully glycosylated mucin binds greater than 40-fold more galectin-3 than mucin from the cells in which oligosaccharide synthesis is blocked at the stage of addition of β3-linked galactose to the N-acetylgalactosamine (Tn antigen) to form T antigen. We reasoned that if T antigen is in fact interacting with galectin-3, then both T antigen-masking and T antigen-mimicking compounds should specifically inhibit this interaction. To test this hypothesis, we performed inhibition ELISA experiments in which T antigen conjugated to HSA was preabsorbed on plastic in 96-well plates, and incubated with purified recombinant human galectin-3 in the presence of different concentrations of the P-30 peptide or lactulosyl-L-leucine. We found that both compounds inhibited galectin-3 binding to T antigen-HSA

conjugate in a dose-dependent manner (Fig. 4, A, B). Although the effect of both compounds was saturable, neither one reached 100% inhibition. We attribute the remaining binding (~30%) to cooperative interactions characteristic of galectin-3[15]. To the best of our knowledge, this is the first observation that directly demonstrated galectin-3 binding to protein-linked T antigen. These data also confirm the specificity of both inhibitors tested, T antigen-masking P-30 peptide, and T antigen-mimicking lactulosyl-L-leucine.

The role of galectin-3 in prostate cancer cell adhesion was recently challenged, however, by the results reported by Ellerhorst et al.[2]. They demonstrated that galectin-3 is not present on the cell surface in any of the four prostate cancer lines they tested, including DU-145, which was used in our experiments, and PC-3, which was shown by another group to bind to the endothelium in a galectin-3-dependent manner[4]. To clarify this issue, we investigated cellular distribution of the galectin-3 during cancer-endothelial cell interaction.

Cellular Distribution of Galectin-3 During Cancer Cell Adhesion to the Endothelium. Laser scanning confocal microscopy was used to study the localization of the galectin-3 in both cancer and endothelial cells upon their interaction. This technique allowed us to analyze the orthogonal plans (XZ and YZ sections), which included both cancer and endothelial cells, as well as the sites of their contact. The results of these experiments (Fig. 5, A, B) revealed remarkably similar patterns of galectin-3 distribution during DU-145 prostate carcinoma (Fig. 5, A) and MDA-MB-435 breast carcinoma (Fig. 5, B) cell adhesion to HUVEC. In both cancer cell lines, galectin-3, although expressed at higher levels than in endothelial cells, remained predominantly intracellular. This

result is in agreement with observations of Ellerhorst et al.[2], and suggests that galectin-3 of cancer cells does not actively participate in their adhesion to the endothelium. In contrast, on endothelial cells we observed the mobilization and clustering of this carbohydrate-binding protein toward the cancer-endothelial cell contacts. This phenomenon is consistent with the interaction of endothelium-expressed galectin-3 with T antigen displayed on the surface of cancer cells, and is indicative of its active role in cancer-endothelial cell adhesion. These results also provide a feasible explanation of why PC-3 cells, which do not exhibit galectin-3 on a cell surface[2], interact with endothelium in a galectin-3 dependent manner, as reported by Lehr & Pienta[4].

The fact that endothelium-expressed galectin-3 clustered toward the sites of cancer-endothelial cell contacts obviously attracted our attention. Thus, we decided to investigate if T antigen was a factor causing galectin-3 mobilization and clustering. We studied the changes in galectin-3 surface expression on endothelial cells after treatment with T antigen-bearing glycoproteins, asialofetuin (ASF), and T antigen-human serum albumin conjugate (T-HSA). Both ASF and T-HSA display multiple immunoreactive T antigen epitopes. Two other proteins, bovine fetuin and human serum albumin (HSA) were used as corresponding negative controls in these experiments. Bovine fetuin is identical to asialofetuin and also contains multiple T antigen antennas, which are, however, covalently masked with sialic (neuraminic) acid and nonimmunoreactive. HSA does not contain T antigen in any form. These experiments revealed that treatment with either ASF (Fig. 5, C) or T-HSA (Fig. 5, D) resulted in rapid and significant increase in galectin-3 expression on a surface of endothelial cells, whereas neither fetuin nor HSA effected this expression. These results demonstrate that T antigen is acting not only as a

12

ligand for galectin-3, but also as a factor causing the mobilization of this carbohydrate-binding protein to the cell surface. The latter observation in turn suggests an important novel function for the circulating cancer mucin, which is often found in serum of patients with adenocarcinomas of different origin[38,39]. Circulating cancer mucin, similar to ASF and T-HSA, bears multiple T antigen moieties, and may likewise induce the increase in galectin-3 surface expression on endothelial cells, thus priming vasculatory endothelium for binding the circulating metastatic tumor cells. Importantly, this phenomenon could be observed when highly metastatic T antigen-expressing MDA-MB-435 cells interact with microvascular endothelium under conditions of flow[32]. In contrast, the MDA-MB-468 cells, which are deficient in T antigen expression and are non-metastatic, do not induce galectin-3 surface mobilization. This observation implies that T antigen-expressing circulating metastatic cancer cells could themselves change endothelium adhesiveness.

The fact that T antigen can actually modify the adhesive properties of the endothelium by mobilizing cell surface adhesion molecules such as galectin-3, adds new and important insights into our understanding of tumor-endothelial cell interactions. It suggests the existence of an additional priming stage in adhesion of circulating metastatic cells to the endothelium, which precedes the docking (initial reversible adhesion) and locking (permanent irreversible adhesion) stages (Fig. 6).

The results presented in this paper identify T antigen as a major cancer cell surface carbohydrate ligand for galectin-3. Although, both the former and the latter may also interact with other cognate ligands, the T antigen-galectin-3 interactions are likely to play a leading role in the initial stages of cancer cell adhesion to the endothelium. The efficient intervention with cancer cell endothelium interactions could result in the

development of new anti-adhesive cancer therapies (reviewed in ref. 40), the concepts of which were brought about by early pioneering works of Dr. R. Kerbel and colleagues[41,42], and Dr. A. Raz and colleagues[43]. The significant inhibition of breast and prostate cancer cell adhesion to the endothelium by T antigen-masking and T antigen-mimicking compounds suggests their high potential to be developed into efficacious antimetastatic agents.

Materials and Methods

Antibodies, Chemicals, and Reagents. The monoclonal anti-T antigen antibody was developed as described[44]. The TIB-166 hybridoma, producing rat monoclonal anti-galectin-3 (anti-Mac-2) was purchased from ATCC. Goat Texas Red-conjugated anti-rat antibody was purchased from Molecular Probes (Eugene, OR). The monoclonal antibody to irrelevant plant protein was kindly provided by the Cell and Immunobiology Core (University of Missouri, Columbia, MO). The *E. coli* strains, expressing human galectin-3 from pET5 vector, were kindly provided by Dr. A. Raz (Wayne State University, Detroit, MI) and Dr. H. Leffler (Lund University, Lund, Sweden). Recombinant human galecin-3 was isolated and affinity purified as described[45]. DiI, 1,1'-dioctadecyl-3, 3, 3', 3'-tetramethylindocarbocyanine was from Molecular Probes, Eugene, OR. Biotinylated T antigen-polyacrylamide conjugate (T-PAA) was from Glycotech Corporation (Rockvill, MD). T antigen-human serum albumin conjugate (T-HSA) was from Dextra Laboratories (Reading, UK). T antigen binding peptide P-30 (HGRFILPWWYAFSPS) and control peptide (RRLLFYKYVYKRYRAGKQRG) were chemically synthesized using FMOC-based chemistry and purified to homogeneity on a C-18 reverse-phase

14

HPLC column (ISCO, Corp.). All other chemicals and reagents, unless otherwise specified, were purchased from Sigma (St. Louis, MO).

Cell Lines and Cultures. The MDA-MB-435 human breast carcinoma cell line was kindly provided by Dr. J. Price (M.D. Anderson Cancer Center, Houston, TX). The DU-145 human prostate carcinoma cells were obtained from American Type Culture Collection (Rockville, MD). B16-F10, a highly metastatic variant of B16-F1 mouse melanoma, was kindly provided by Dr. I. Fidler (M.D. Anderson Cancer Center, Houston, TX). The RPMI-1640 medium supplemented with L-glutamine, 10% fetal bovine serum (FBS), sodium pyruvate, and non-essential amino acids, was used for all tumor cell lines.

Human umbilical vein endothelial cells (HUVEC) were purchased from Cascade Biologics (Portland, OR). The basal Medium 200 (Cascade Biologics) supplemented with low serum growth supplement (LSGS) containing FBS (2% v/v final concentration), hydrocortisone, human fibroblast growth factor, heparin, and human epidermal growth factor was used for HUVEC. The cells at population doublings of approximately 8-12 were used for the adhesion experiments.

All cells were maintained on plastic as a monolayer culture in a humidified incubator in 5% CO_2/95% air at 37°C.

Adhesion to the Endothelium. The adhesion experiments were performed exactly as described[11]. A single cell suspension of cancer cells prelabeled with 3 μg/ml solution of acridine orange or 5 μg/ml solution of DiI in RPMI-1640 media ($5·10^4$ cell per chamber in

2.5 ml of complete media supplemented with various concentrations of the compound tested) was added to the monolayer of the endothelial cells grown to confluence directly on microscope slides using 4-well chamber slides (NalgeNunc, Naperville, IL). The chambers were sealed, and cells were allowed to adhere for 1 h at 37°C, after which the chambers were inverted and left upside-down for 30 min to allow sedimentation of nonadhered cells. After that, the medium was drained, samples were gently rinsed with PBS, fixed for 30 min in 2% formaldehyde solution in PBS, mounted under cover glass, and examined by fluorescent microscopy. Four random fields in each well were photographed at 250x magnification and the total number of adhered cells in every field was counted. The assay was performed in quadruplicate for each condition.

T Antigen Cell Binding Assay. The B16-F10 mouse melanoma cell line was selected for these experiments because it does not expresses T antigen[22], which could interfere with the assay, but is capable of binding T antigen, as reflected by its interaction with asialofetuin[23]. The cells were placed on a microscope slide, fixed for 30 min in 2% formaldehyde solution in PBS, and incubated for 1 h in PBS containing biotinylated T antigen-PAA conjugate (20 µg/ml final concentration) with or without lactulosyl-L-leucine (2 mM final concentration) at room temperature. Cells were washed three times with PBS. Bound T-PAA was visualized using peroxidase-labeled streptavidin and DAB as a chromogenic substrate. After counterstaining with hematoxylin, samples were mounted under cover glass and analyzed microscopically at 900x magnification.

Dot Blot Assay. Bovine asialofetuin, bearing multiple T antigen epitopes, was immobilized on the nitrocellulose membrane (1 µg per spot). After blocking with 2% solution of BSA in TBS, samples were incubated for 1 h at room temperature with different concentrations of peroxidase-labeled T antigen-specific PNA lectin without (control) or with addition of 2 mM (final concentration) of lactulosyl-L-leucine or lactitol-L-leucin in 2% BSA solution in TBS. The membranes were washed 3x10 min in TBS and developed with DAB.

Inhibition ELISA. T antigen-human serum albumin conjugate (250 ng/well) was preabsorbed to 96-well plates overnight, blocked with 1% solution of BSA in PBS, and incubated for 1 h with 10 µg/ml solution of purified galectin-3 (1 µg/well) in the presence of different concentrations of T antigen-specific P-30 peptide (0-50 µM) or lactulosyl-L-leucine (0-1 mM) at room temperature. Bound galectin-3 was detected by sequential incubation with rat anti-galectin-3 monoclonal antibody, alkaline phosphatase conjugated goat anti-rat IgG, and p-nitrophenyl phosphate, followed by reading the absorbance at 405 nm. The plates were washed three times with PBS between steps. Controls containing no galectin-3 were included as blanks. Data represent the results of at least three determinations for each condition. The inhibition percent was calculated as a decrease in the mean net absorbance at 405 nm compared to control.

Cytochemistry, Laser Scanning Confocal Microscopy, and Immunofluorescence. The cytochemical analysis of T antigen was performed using peanut lectin-horseradish

17

peroxidase conjugate (PNA-HRP) and subsequent color reaction with diaminobenzidine (DAB).

The samples for the analysis of galectin-3 cellular distribution were prepared exactly as described in adhesion to the endothelium, except that cancer cells were not prelabeled, and samples were fixed and permeabilized in 4% formaldehyde solution in PBS for 24 h. The rat anti-galectin-3 and goat Texas Red-conjugated anti-rat antibodies were used to visualize galectin-3. The laser scanning confocal microscopy was performed on a Bio-Rad MRC 600 confocal system. The Z stacks were prepared by obtaining serial sections with 0.5 μm increments and analyzed in orthogonal projections (Y-Z and X-Z sections) using the MetaMorph Immaging System software (Universal Imaging, Hallis, NH).

To evaluate cell surface galectin-3 expression, live, nonfixed, and nonpearmabilized endothelial cells, grown to confluence directly on microscope slides, were incubated for 45 min at 37°C in complete media supplemented with rat anti-galectin-3 antibody without (control) or with 1 mg/ml (final concentration) of bovine fetuin or ASF, or 0.5 mg/ml (final concentration) of HSA or T-HSA. Slides were washed three times with PBS and incubated for 1 h with goat Texas Red-conjugated anti-rat antibody. After additional washes the samples were mounted under cover glass and analyzed on a Bio-Rad MRC 600 confocal system using accumulation of four scans. The 4-well slides (NalgeNunc, Naperville, IL) were used, which allowed simultaneous processing of samples to be compared. The exact same conditions such as iris settings, laser intensity, gain, magnification, and number of scan accumulations were used for all samples.

References

1. Al-Mehdi, A.B., Tozawa, K., Fisher, A.B., Shientag, L., Lee, A., and Muschel, R.J. Intravascular origin of metastasis from the proliferation of endothelium-attached tumor cells: a new model for metastasis. *Nat. Med.* **6**, 100-102 (2000).

2. Ellerhorst, J., Nguyen, T., Cooper, D.N.W., Lotan, D., and Lotan, R. Differential expression of endogenous galectin-1 and galectin-3 in human prostate cancer cell lines and effects of overexpressing galectin-1 on cell phenotype. *Int. J. Oncology* **14**, 217-224 (1999).

3. Lawrence, M.B., and Springer, T.A. Leukocytes roll on a selectin at physiologic flow rates: distinction from and prerequisite for adhesion through integrins. *Cell* **65**, 859-873 (1991).

4. Lehr, J.E., and Pienta, K.J. Prefential adhesion of prostate cancer cells to a human bone marrow endothelial cell line. *J. Natl. Cancer Inst.* **90**, 118-123 (1998).

5. Hakomori, S-I. Aberrant glycosylation in tumors and tumor-associated carbohydrate antigens. *Adv. Cancer Res.* **52,** 257-331 (1989).

6. Hakomori, S-I. Possible functions of tumor associated carbohydrate antigens. *Curr. Opin. Immunol.* **48,** 665-673 (1983).

7. Springer, G.F., Desai, P.R., Ghazizadeh, M., and Tegtmeyer, H. T/Tn pancarcinoma autoantigens: fundamental, diagnostic and prognostic aspects. *Cancer Detect. Prev.* **19,** 173-182 (1995).

8. Fonseca, I., Costa Rosa, J., Felix, A., Therkildsen, M.H., and Soares, J. Simple mucin-type carbohydrate antigens (T, Tn and sialosyl-Tn) in mucoepidermoid carcinoma of the salivary glands. *Histopathology* **25,** 537-543 (1994).

9. Springer, G.F., Cheingsong-Popov, R., Schirrmacher, V., Desai, P.R., and Tegtmeyer, H. Proposed molecular basis of murine tumor cell-hepatocyte interaction. *J. Biol. Chem.* **258,** 5702-5706 (1983).

10. Janssen, T., Petein, M., Van Velthoven, R., Van Leer, P., Fourmarier, M., Vanegas, J.P., Danguy, A., Schulman, C., Pasteels, J.L., and Kiss, R. Differential histochemical peanut agglutinin stain in benign and malignant human prostate tumors: relationship with prostatic specific antigen immunostain and nuclear DNA content. *Hum. Pathol.* **12,** 1341-1347 (1996).

11. Glinsky, V.V., Huflejt, M.E., Glinsky, G.V., Deutscher, S.L., and Quinn, T.P. Effects of Thomsen-Friedenreich antigen-specific peptide P-30 on β-galactoside-mediated homotypic aggregation and adhesion to the endothelium of MDA-MB-435 human breast carcinoma cells. *Cancer Res.* **60,** 2584-2588 (2000).

12. Sparrow, C.P., Leffler, H., and Barondes, S.H. Multiple soluble β-galactoside-binding lectins from human lung. *J. Biol. Chem.* **262,** 7383-73-90 (1987).

13. Barondes, S.H., Castranovo, V., Cooper, D.N., Cummings, R.D., Drickamer, K., Feizi, T., Gitt, M.A., Hirabayashi, J., Hughes, C., Kasai, K., Leffler, H., Liu, F.T., Lotan, R., Mercurio, M.N., Monsigny, M., Pillai, S., Poirer, F., Raz, A., Rigby, P.W.J., Rini, J.M., and Wang, J.L. Galectins: a family of animal β-galactoside-binding lectins. *Cell* **76,** 597-598 (1994).

14. Dagher, S.F., Wang, J.L., and Patterson, R.J. Identification of galectin-3 as a factor in pre-mRNA splicing. *Proc. Natl. Acad. Sci. USA* **92,** 1213-1217 (1995).

15. Barondes, S.H., Cooper, D.N.W., Gitt, M.A., and Leffler, H. Galectins, structure and function of a large family of animal lectins. *J. Biol. Chem.* **269,** 20807-20819 (1994).

16. Akahani, S., Nangia-Makker, P., Inohara, H., Kim, H-R.C., and Raz, A. Galectin-3: a novel antiapoptotic molecule with a functional BH1 (NWGR) domain of Bcl-2 family. *Cancer Res.* **57,** 5272-5276 (1997).

17. Kim, H-R.C., Lin, H-M., Biliran, H., and Raz, A. Cell cycle arrest and inhibition of anoikis by galectin-3 in human breast epithelial cells. *Cancer Res.* **59,** 4148-4154 (1999).

18. Inohara, H., and Raz, A. Functional evidence that cell surface galectin-3 mediates homotypic cell adhesion. *Cancer Res.* **55,** 3267-3271 (1995).

19. Inohara, H., Akahani, S., Koths, K., and Raz, A. Interactions between galectin-3 and Mac-2-binding protein mediate cell-cell adhesion. *Cancer Res.* **56,** 4530-4534 (1996).

20. Nangia-Makker, P., Sarvis, R., Visscher, D.W., Baily-Penrod, J., Raz, A., and Sarkar, F.H. Galectin-3 and L1 retrotransposons in human breast carcinomas. *Cancer Res. Treat.* **49,** 171-183 (1998).

21. Nangia-Makker, P., Thompson, E., Hogan, C., Ochieng, J., and Raz, A. Induction of tumorigenicity by galectin-3 in a non-tumorigenic human breast carcinoma cell line. *Int. J. Oncol.* **7,** 1079-1087 (1995).

22. Peletskaya, E.N., Glinsky, G.V., Deutscher, S.L., and Quinn, T.P. Identification of peptide sequences that bind the Thomsen-Friedenreich cancer-associated glycoantigen from bacteriophage peptide display libraries. *Molecular Diversity* **2,** 13-18 (1996).

23. Peletskaya, E.N., Glinsky, V.V., Glinsky, G.V., Deutscher, S.L., and Quinn, T.P. Characterization of peptides that bind the tumor-associated Thomsen-Friedenreich antigen selected from bacteriophage display libraries. *J. Mol. Biol.* **270,** 374-384 (1997).

24. Wolf, M.F., Ludwig, A., Fritz, P., and Schumacher, K. Increased expression of Thomsen-Friedenreich antigens during tumor progression in breast cancer patients. *Tumour Biol.* **9,** 190-194 (1988).

25. Ghazizadeh, M., Kagawa, S., Izumi, K., and Kurokawa, K. Immunohistochemical localization of T antigen-Like substance in benign hyperplasia and adenocarcinoma of the prostate. *J. Urol.* **132,** 1127-1130 (1984).

26. Honn, K.V., & Tang, D.G. Adhesion molecules and tumor cell interaction with endothelium and subendothelial matrix. *Cancer Metastasis Rev.* **11,** 353-375 (1992).

27. McClay, D.R., Wessel, G.M., & Marchase, R.B. Intercellular recognition: Quantitation of initial binding events. *Proc. Natl. Acad. Sci. USA* **78,** 4975-4979 (1981).

28. Zhang, R.D., Fidler, I.J., and Price, J.E. Relative malignant potential of human breast carcinoma cell lines established from pleural effusion and a brain metastasis. *Invasion & Metastasis,* **11,** 204-215 (1991).

29. Price, J.E., Polyzos, A., Zhang, R.D., and Daniels, L.M. Tumrigenicity and metastasis of human breast carcinoma cell lines in nude mice. *Cancer Res.,* **50,** 717-721 (1990).

30. Stone, K.R., Mickey, D.D., Wunderli, H., Mickey, G.H., & Paulson, D.F. Isolation of human prostate carcinoma cell line (DU-145). *Int. J. Cancer,* **21,** 274-281 (1978).

31. Bladou, F., Gleave, M.E., Penault-Llorca, F., Serment, G., Lange, P.H., & Vessella, R.L. In vitro and in vivo models developed from human prostatic cancer. *Prog. Urol.,* **7,** 384-396 (1997).

32. Khaldoyanidi, S.K., Glinsky, V.V., Sikora, L., Glinskii, A.B., Mossine, V.V., Glinsky, G.V., Sriramarao, P. Role of galectin-3 in homo- and heterotypic intercellular adhesion of human metastatic breast carcinoma cells to endothelia under flow conditions. *Submitted.* (2000)

33. Glinsky, G.V., Mossine, V.V., Price, J.E., Bielenberg, D., Glinsky, V.V., Ananthaswamy, H.N., & Feather, M.S. Inhibition of colony formation in agarose of metastatic breast carcinoma and melanoma cells by synthetic glycoamine analogs. *Clin. Exp. Metastasis* **14,** 253-267 (1996).

34. Glinsky, G.V., Price, J.E., Glinsky, V.V., Mossine, V.V., Kiriakova, G., & Metcalf, J.B. Inhibition of human breast cancer metastasis in nude mice by synthetic glycoamines. *Cancer Res.* **56,** 5319-5324 (1996).

35. Raz, A., & Lotan, R. Endogenous galactoside-binding lectins: a new class of functional tumor cell surface molecules related to metastasis. *Cancer Metastasis Rev.* **6,** 433-452 (1987).

36. Lotan, R., & Raz, A. Endogenous lectins as mediators of tumor cell adhesion. *J. Cell. Biochem.* **37,** 107-117 (1988).

37. Lotan, R., Belloni, P.N., Tressler, R.J., Lotan, D., Xu, X-C., & Nicolson, G.L. Expression of galectins on microvessel endothelial cells and their involvement in tumor cell adhesion. *Glycoconjugate J.* **11,** 462-468 (1994).

38. Bresalier, R.S., Byrd, J.C., Wang, L., & Raz, A. Colon cancer mucin: A new ligand for the β-galactoside-binding protein galectin-3. *Cancer Res.* **56,** 4354-4357 (1996).

39. Duffy, M.J., CA 15-3 and related mucins as circulating markers in breast cancer. *Ann. Clin. Biochem.* **(Pt 5),** 579-586 (1999).

40. Glinsky, G.V., Anti-adhesion cancer therapy. *Cancer Metastasis Rev.,* **17,** 177-185 (1998).

41. Kerbel, R.S., St. Croix, B., Rak, J., & Graham, C.H. Is there a role for anti-adhesives as chemosensitizers in the treatment of solid tumors by chemotherapy? *Bull. Inst. Pasteur* **92,** 248-256 (1995).

42. Kerbel, R.S., St. Croix, B., Florenes, V.A., & Rak, J. Induction and reversal of cell adhesion-dependent multicellular drug resistance in solid breast tumors. *Hum. Cell* **9,** 257-264 (1996).

43. Inohara, H. & Raz, A. Effects of natural complex carbohydrate (citrus pectin) on murine melanoma cell properties related to galectin-3 functions. *Glycoconj. J.* **11,** 527-532 (1994).

44. Rittenhouse-Diakun, K., Xia, Z., Pickhardt, D., Morey, S., Baek, M.-G., and Roy, R. Development and characterization of monoclonal antibody to T-antigen: (Galβ1-3GalNAc-α-O). *Hybridoma* **17,** 165-173 (1998).

45. Ochieng, J., Platt, D., Tait, L., Hogan, V., Raz, T., Carmi, P., and Raz, A. Structure-function relationship of a recombinant human galactoside-binding protein. *Biochemistry* **32,** 4455-4460 (1993).

Figures Legends

Figure 1. Expression of T antigen in a human prostate cancer lesion (A) and in DU-145 human prostate adenocarcinoma cell line (B) as revealed by binding of T antigen-specific PNA lectin-horseradish peroxidase conjugate followed by color reaction with diaminobenzidine tetrahydrochloride. Brown color indicates the presence of immunoreactive T antigen.

Figure 2. Dose-dependent inhibition of DiI- (A) and acridine orange- (B-G) labeled DU-145 human prostate carcinoma cell adhesion to the endothelium by sythetic T antigen-specific P-30 peptide, but not by the control peptide (H). In B through H, numbers at the bottom of the photomicrographs indicate concentration of the peptide tested. I, J, maximal inhibitory effect on adhesion of MDA-MB-435 human breast

carcinoma (I) and DU-145 human prostate carcinoma (J) cells to the endothelium

achievable with anti-T antigen monoclonal antibody and P-30 peptide. *Error bars,* SD.

Figure 3. T antigen-mimicking lactulosyl-L-leucine competes off (C) biotinylated T

antigen-PAA conjugate bound to the B16-F10 mouse melanoma cells (B). A, control

sample counterstained with hematoxylin. D, inhibition of T antigen-specific PNA lectin

binding to asialofetuin (iv) by T antigen-mimicking lactulosyl-L-leucine (v), but not by

lactitol-L-leucine (vi); i-iii, binding of different concentrations of PNA lectin to

asialofetuin (1 μg) spotted on the nitrocellulose membrane. E-G, inhibition of DiI-

labeled MDA-MB-435 breast carcinoma cell adhesion to the endothelium by T antigen-

mimicking lactulosyl-L-leucine (F), but not by lactitol-L-leucine (G), compared with the

control (E).

Figure 4. Dose-dependent inhibition of recombinant human galectin-3 binding to T

antigen-HSA conjugate by T antigen-masking P-30 peptide, and T antigen-mimicking

lactulosyl-L-leucine. The inhibition percent was calculated as a decrease in the mean net

absorbance at 405 nm compared to the control. *Bars,* SD.

Figure 5. A, B, pseudocolored XZ sections showing cellular distribution of galectin-3

upon adhesion of DU-145 prostate (A), and MDA-MB-435 breast (B) cancer cells to the

endothelium. Different colors represent different concentrations of galectin-3 (purple,

blue, green, yellow, red, and white, from lowest to highest). Note the accumulation and

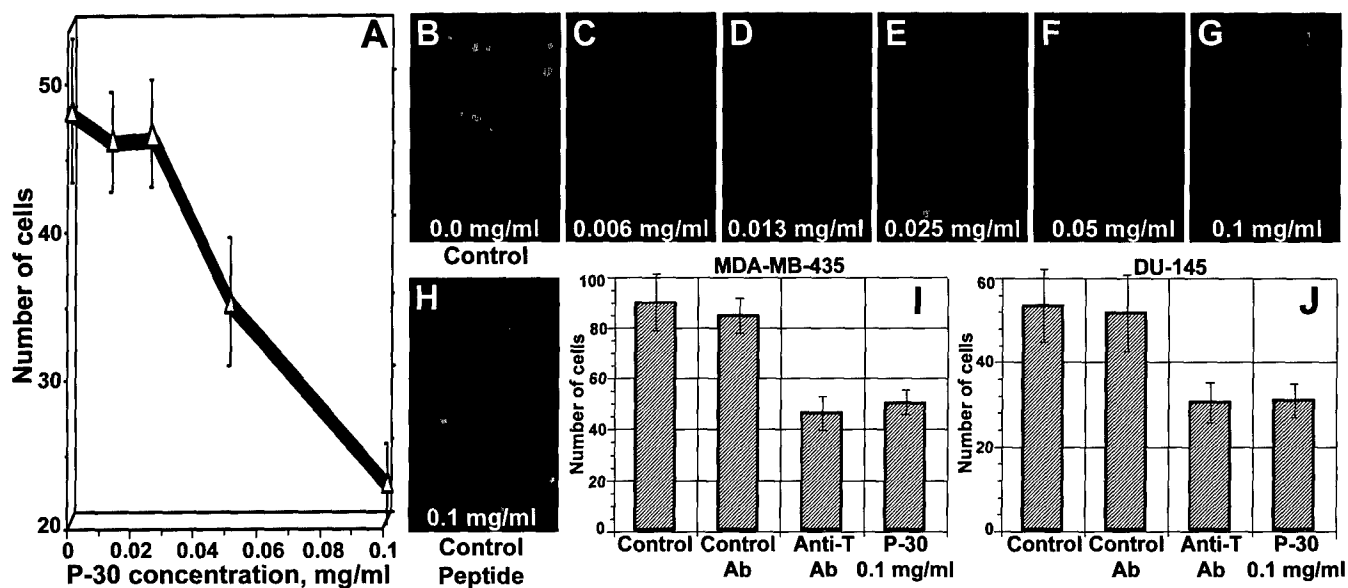clustering of galectin-3 toward cell contacts on endothelial cells indicated by arrows,

whereas in cancer cells the protein remains predominantly intracellular. C, D, the effect

of asialofetuin (ASF) and T antigen-HSA conjugate (T-HSA) on galectin-3 surface

expression on endothelial cells. Note the increase in galectin-3 surface representation

upon treatment with ASF (C) or T-HSA (D), but not with fetuin or HSA, compared with

the control. In both C and D top panel shows corresponding transmitted light

photomicrograph of the same field.

Figure 6. Schematic representation of T antigen participation in adhesion of metastatic

cancer cells to the vasculatory endothelium. Circulating T antigen-bearing cancer-

associated glycoproteins and metastatic tumor cells induce the mobilization of the

galectin-3 to the surface of endothelial cells (priming stage). T antigen-expressing

malignant cells bind to the endothelium through T antigen-galectin-3 interactions

(docking stage) allowing sufficient time for the stabilizing integrin-mediated adhesion
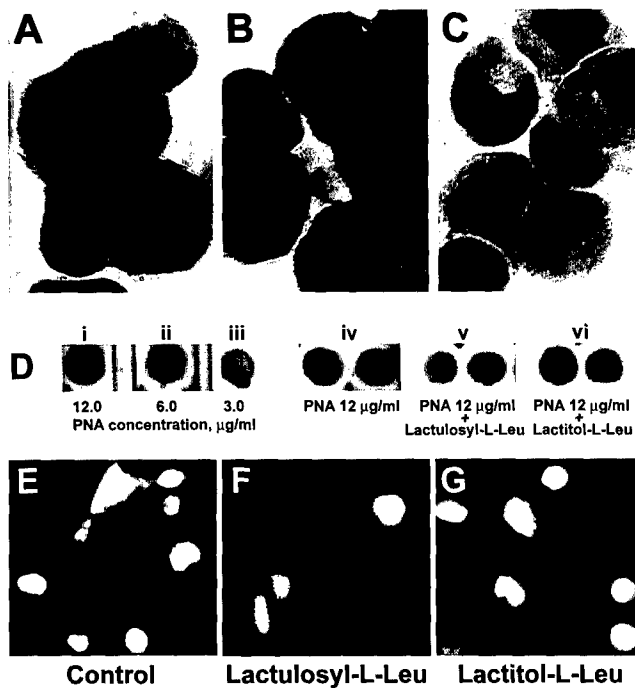
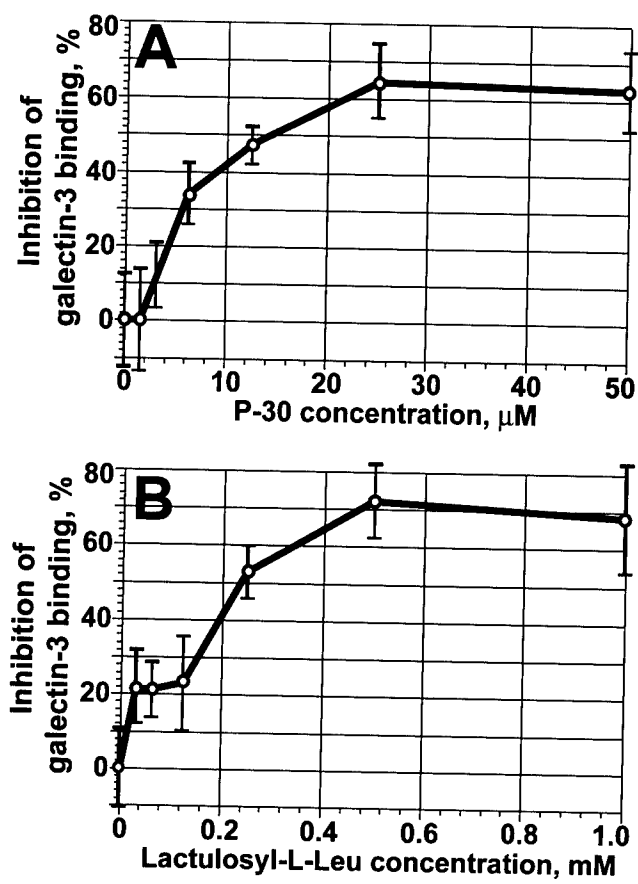events to take place (locking stage).
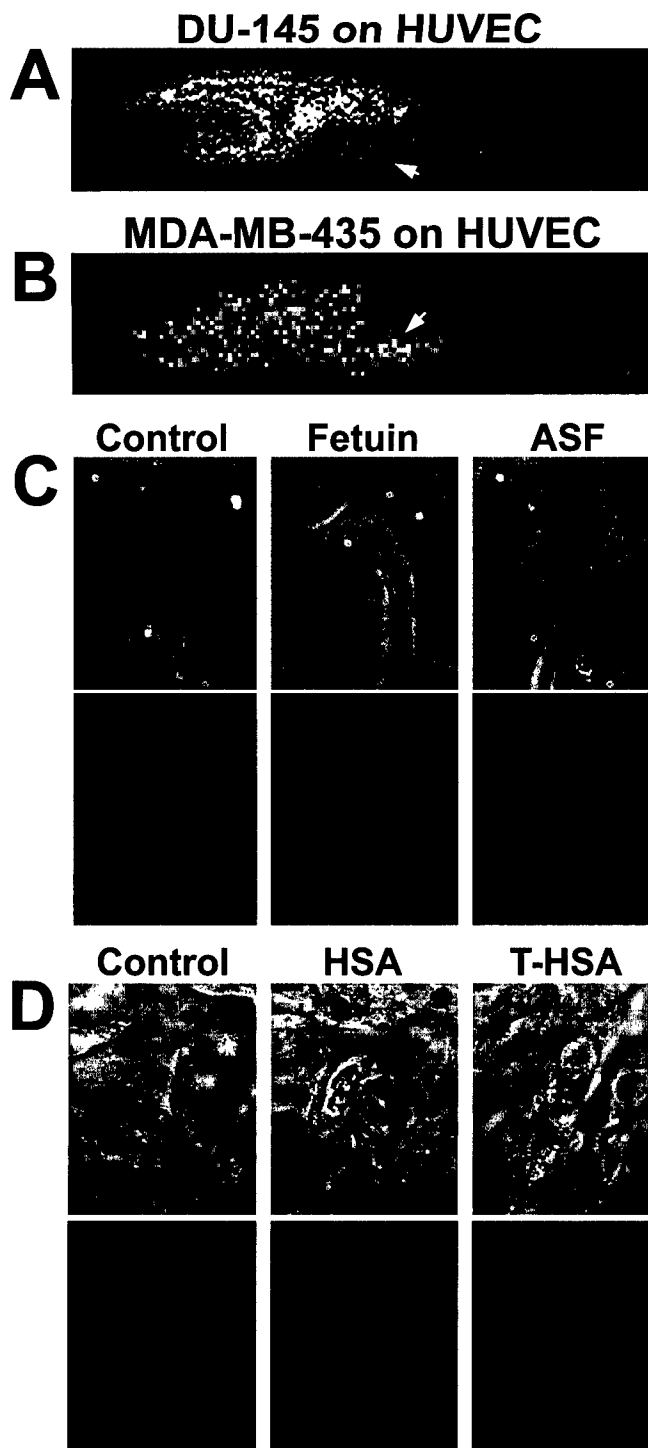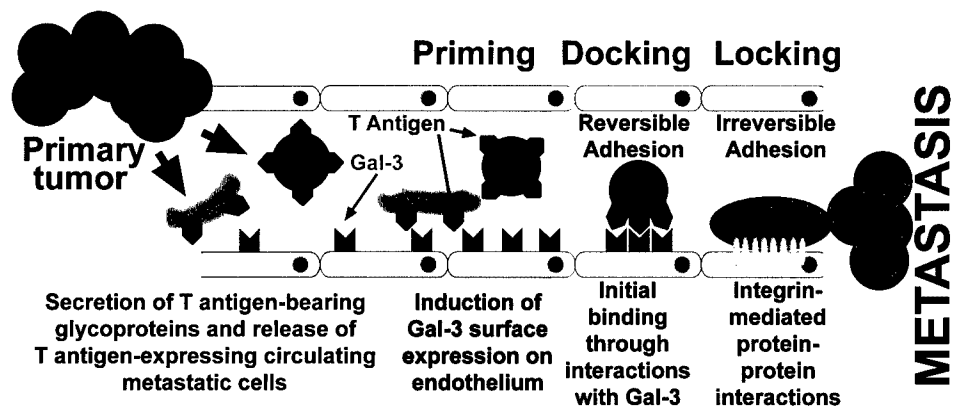
FIGURE 1

FIGURE 2

FIGURE 3

FIGURE 4

FIGURE 5

A
DU-145 on HUVEC

B
MDA-MB-435 on HUVEC

C
| Control | Fetuin | ASF |

D
| Control | HSA | T-HSA |

FIGURE 6

Priming   Docking   Locking

T Antigen

Gal-3

| Reversible Adhesion | Irreversible Adhesion |

Primary tumor

Secretion of T antigen-bearing glycoproteins and release of T antigen-expressing circulating metastatic cells

Induction of Gal-3 surface expression on endothelium

Initial binding through interactions with Gal-3

Integrin-mediated protein-protein interactions

METASTASIS

REPLY TO
ATTENTION OF:

MCMR-RMI-S   (70-1y)   23 Aug 01

MEMORANDUM FOR Administrator, Defense Technical Information
Center (DTIC-OCA), 8725 John J. Kingman Road, Fort Belvoir,
VA 22060-6218

SUBJECT: Request Change in Distribution Statement

1. The U.S. Army Medical Research and Materiel Command has
reexamined the need for the limitation assigned to the technical
reports listed at enclosure. Request the limited distribution
statement for these reports be changed to "Approved for public
release; distribution unlimited." These reports should be
released to the National Technical Information Service.

2. Point of contact for this request is Ms. Judy Pawlus at
DSN 343-7322 or by e-mail at judy.pawlus@det.amedd.army.mil.

FOR THE COMMANDER:

Encl   PHYLIS M. RINEHART
                                            Deputy Chief of Staff for
                                              Information Management

Reports to be Downgraded to Unlimited Distribution

ADB241560	ADB253628	ADB249654	ADB263448
ADB251657	ADB257757	ADB264967	ADB245021
ADB263525	ADB264736	ADB247697	ADB264544
ADB222448	ADB255427	ADB263453	ADB254454
ADB234468	ADB264757	ADB243646	
ADB249596	ADB232924	ADB263428	
ADB263270	ADB232927	ADB240500	
ADB231841	ADB245382	ADB253090	
ADB239007	ADB258158	ADB265236	
ADB263737	ADB264506	ADB264610	
ADB239263	ADB243027	ADB251613	
ADB251995	ADB233334	ADB237451	
ADB233106	ADB242926	ADB249671	
ADB262619	ADB262637	ADB262475	
ADB233111	ADB251649	ADB264579	
ADB240497	ADB264549	ADB244768	
ADB257618	ADB248354	ADB258553	
ADB240496	ADB258768	ADB244278	
ADB233747	ADB247842	ADB257305	
ADB240160	ADB264611	ADB245442	
ADB258646	ADB244931	ADB256780	
ADB264626	ADB263444	ADB264797	

Encl